

This article was downloaded by:

On: 15 January 2011

Access details: *Access Details: Free Access*

Publisher *Taylor & Francis*

Informa Ltd Registered in England and Wales Registered Number: 1072954 Registered office: Mortimer House, 37-41 Mortimer Street, London W1T 3JH, UK



## Comments on Inorganic Chemistry

Publication details, including instructions for authors and subscription information:

<http://www.informaworld.com/smpp/title~content=t713455155>

## Organometallic Sandwich Compounds in Layered Lattices

Dermot O'hare<sup>a</sup>; John S. O. Evans<sup>a</sup>

<sup>a</sup> Inorganic Chemistry Laboratory, University of Oxford, Oxford, United Kingdom

**To cite this Article** O'hare, Dermot and Evans, John S. O.(1993) 'Organometallic Sandwich Compounds in Layered Lattices', *Comments on Inorganic Chemistry*, 14: 2, 155 – 206

**To link to this Article:** DOI: 10.1080/02603599308048660

**URL:** <http://dx.doi.org/10.1080/02603599308048660>

PLEASE SCROLL DOWN FOR ARTICLE

Full terms and conditions of use: <http://www.informaworld.com/terms-and-conditions-of-access.pdf>

This article may be used for research, teaching and private study purposes. Any substantial or systematic reproduction, re-distribution, re-selling, loan or sub-licensing, systematic supply or distribution in any form to anyone is expressly forbidden.

The publisher does not give any warranty express or implied or make any representation that the contents will be complete or accurate or up to date. The accuracy of any instructions, formulae and drug doses should be independently verified with primary sources. The publisher shall not be liable for any loss, actions, claims, proceedings, demand or costs or damages whatsoever or howsoever caused arising directly or indirectly in connection with or arising out of the use of this material.

## Organometallic Sandwich Compounds in Layered Lattices

DERMOT O'HARE and JOHN S. O. EVANS

*Inorganic Chemistry Laboratory,  
University of Oxford,  
South Parks Road,  
Oxford, OX1 3QR,  
United Kingdom*

Received August 11, 1992

The intercalation of organometallic guest molecules between the sheets of layered inorganic host lattices has attracted a considerable amount of research over the past 18 years. The process of intercalation has been found to dramatically alter the bulk properties of these materials, and there has been much interest in their conductivity, optical, catalytic and magnetic properties. Nevertheless, fundamental questions regarding the orientational preferences and the redox states of sandwich compounds intercalated in these layer hosts have been the subject of considerable debate in the recent literature. The introduction of organometallic species, which often have interesting chemistry in their own right and whose steric and electronic properties can be systematically varied via either metal or ring substitution, offers the solid state chemist a unique opportunity to tailor the properties of the resultant material in a controlled manner, and at what are, for solid state reactions, extremely low temperatures. We have reviewed with specific examples the developments in this area, and discuss the current state of the art.

**Key Words:** *intercalation, organometallic, layered lattice, solid state, magnetism, solid state, metallocene, bis(arene)metal*

**Abbreviations Used:** Cp =  $\eta^5\text{-C}_5\text{H}_5$ , CpMe =  $\eta^5\text{-C}_5\text{H}_4\text{Me}$ , Cp\* =  $\eta^5\text{-C}_5\text{Me}_5$ , Cht

*Comments Inorg. Chem.*  
1993, Vol. 14, Nos. 2 & 3, pp. 155–206  
Reprints available directly from the publisher.  
Photocopying permitted by license only

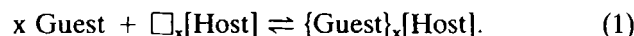
© 1993 Gordon and Breach,  
Science Publishers S.A.  
Printed in Singapore

=  $\eta^7\text{-C}_7\text{H}_7$ , Bz =  $\eta^6\text{-C}_6\text{H}_6$ , Tol =  $\eta^6\text{-C}_6\text{H}_5\text{Me}$ , Mes =  $\eta^6\text{-C}_3\text{H}_3\text{Me}_3$ , Cot =  $\eta^8\text{-C}_8\text{H}_8$

## 1. INTRODUCTION

The first modern day report of an intercalation compound appears to have been inadvertently described by C. Schafhäütl in 1840 when he reported his observations on attempting to dissolve graphite in sulphuric acid.<sup>1</sup> However, the contemporary resurgence of the subject dates from 1926 when Karl Fredenhagen and Gustav Cad-enback described the uptake of potassium vapour into graphite.<sup>2</sup> Since their report, intercalation reactions have been reported by inorganic, organic and organometallic chemists, and to date over 5000 scientific papers have been published describing the synthesis, reactivity, and physical characterisation of inorganic intercalation compounds.

Literally, the term *intercalation* refers to the act of inserting into a calendar some extra interval of time. Today the usage of the term intercalation by chemists is to describe the (reversible) insertion of mobile guest species (atoms, molecules or ions) into a crystalline host lattice that contains an interconnected system of empty lattice sites ( $\square$ ) of appropriate size. The reaction can be generalised by Eq. (1).



As indicated by Eq. (1), intercalation reactions are usually reversible, and they may also be characterised as topochemical processes, since the structural integrity of the host lattice is formally conserved in the course of the forward and reverse reactions. Typically these reactions occur near room temperature, which is in sharp contrast to most conventional solid state synthetic procedures which often require temperatures in excess of 600°C. Remarkably, a wide range of host lattices have been found to undergo these low temperature reactions, including framework (3-D), layer (2-D), and linear chain (1-D) lattices.

In this review we describe the synthesis and our current understanding of the structural and electronic properties of the inter-

calation compounds formed by insertion of sandwich organometallic guests into lamellar host lattices. A prototypical organometallic sandwich compound would be ferrocene, but we have also included metal containing guests containing two  $\pi$ -bonded carbocyclic rings.

## 2. INTERCALATES OF THE TRANSITION METAL DICHALCOGENIDES

The first report of intercalation into a layered transition metal dichalcogenide host came in 1954 when Rüdorff reported that a number of conducting layered disulphides would react with liquid ammonia solutions of alkali metals in a manner analogous to that of graphite.<sup>3</sup> Since then the intercalation of a wide variety of guest species including both solvated and unsolvated metal ions, protons, amines, pyridines, organic species such as the tropylium ion, and organometallic compounds has been reported and reviewed.<sup>4-8</sup>

One of the initial reasons for the sudden growth of interest in these compounds was the discovery that the intercalation of certain guest species could dramatically alter the conductivity properties of the host lattice, and in some cases cause the host lattice to become superconducting.<sup>9-12</sup> Layered systems such as these are of extreme interest in the theoretical study of superconductivity, and one surprising early observation was that the critical temperature,  $T_c$ , of these materials was independent of the interlayer separation, which implies that their superconducting state must be largely two dimensional in nature. These materials have since received attention for their possible application as reversible electrodes in solid state batteries, their potential catalytic properties, and for their unusual physical properties such as their tendency to undergo Peierls lattice distortions and exhibit charge density waves.<sup>6,13</sup>

The structure of the layered metal dichalcogenides consists of sheets of metal ions either octahedrally or trigonally coordinated by sulphur ions. These strongly bonded sheets are then held together by weak Van der Waals forces so as to build up the layer structure (Fig. 1). This possibility of different metal coordination sites, coupled with the fact that the inherent weakness of interlayer forces means that individual layers can stack on top of one another

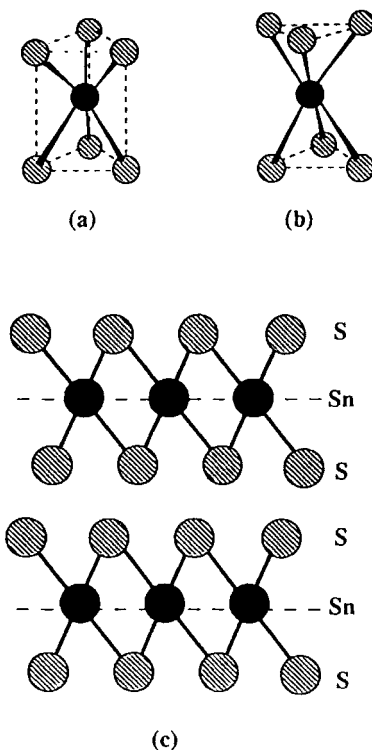


FIGURE 1 The structure of the layered metal dichalcogenides. (a) trigonal prismatic, (b) octahedral coordination of the metal ion, (c) the layered structure of  $2H\ SnS_2$ .

in a number of different ways, gives rise to the frequent observation of polytypism in these compounds. Whilst the number of polytypes observed for the transition metal dichalcogenides is not nearly as large as for compounds such as  $CdI_2$ , one must always be extremely careful in the synthesis of host lattices, as different polytypes can often exhibit different physical properties and consequently very different intercalation chemistry.

In the case of  $TaS_2$  there are a number of major polytypes known. The simplest form is the 1T polytype which contains octahedrally coordinated metal ions. In this nomenclature the "1" refers to the number of individual layers required to describe a

repeat unit, and the "T" to the overall symmetry of the lattice (T is trigonal, H hexagonal). A schematic representation of the  $\{11\bar{2}0\}$ -plane of 1T  $\text{TaS}_2$ , and those of the other common polytypes, is given in Fig. 2.  $\text{TaS}_2$  can also be prepared as the 2H polytype which contains trigonal prismatic metal coordination. This form would initially appear to be less stable than the 1T polytype in that there are additional repulsions present caused by the fact that the chalcogen atoms now lie directly above each other. This destabilisation is, however, compensated by an increase in the stability of the band structure, as trigonal prismatic coordination causes a lowering of the energy band formed by overlap of the Ta  $5d_{z^2}$  orbitals. In fact the energy difference between the two forms is extremely small for  $\text{TaS}_2$ , and the synthesis of a polytypically pure phase can be difficult. Several other polytypes are known, but their organometallic intercalation chemistry is not well developed, and the interested reader is referred elsewhere.<sup>14</sup> The two other dichalcogenides which will be discussed in some depth in this review are 1T  $\text{ZrS}_2$  which is isostructural to 1T  $\text{TaS}_2$  and 2H  $\text{SnS}_2$ , which has the  $\text{CdI}_2$  structure, and again contains octahedrally coordinated metal ions. The metal dichalcogenides were first shown to intercalate organometallic sandwich compounds by M. B. Dines in 1975 in a paper which described the intercalation of cobaltocene  $\{\text{Co}(\text{Cp})_2\}$  and chromocene  $\{\text{Cr}(\text{Cp})_2\}$  into 8 different layered metal dichalcogenides. Since that time, a large number of other sandwich in-

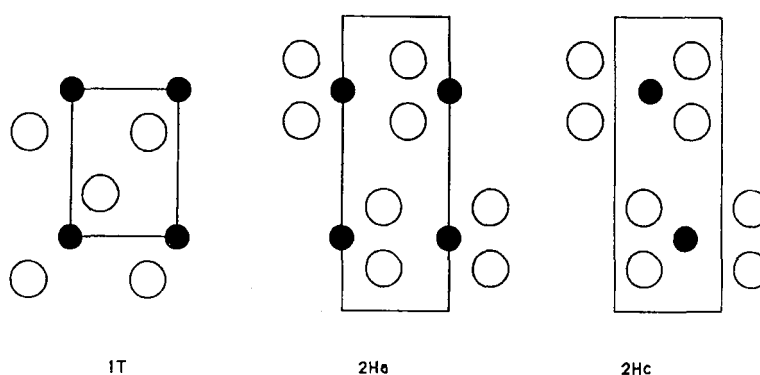


FIGURE 2  $11\bar{2}0$  plane of (a) the 1T, (b) 2Ha, and (c) 2Hc polytypes of  $\text{TaS}_2$ .

tercalation compounds have been synthesised by both direct and ion exchange routes, and they are summarised in Table I.

Despite the fact that there has been considerable research into the structure and properties of these compounds over the past 18 years, there still remains considerable controversy over, in particular, the orientation of these sandwich guest molecules, and the electronic processes which occur between the guest molecules and the host lattice.

TABLE I

A summary of the organometallic sandwich compounds which have successfully been intercalated into layered metal dichalcogenide hosts. \* refers to syntheses in which the product obtained appeared to be impure, and the guest stoichiometry given is almost certainly an overestimate.

| Host Lattice        | Guest                               | Stoichiometry | Interlamellar Separation Å | $\Delta c$ Å | Reference |
|---------------------|-------------------------------------|---------------|----------------------------|--------------|-----------|
| ZrS <sub>2</sub>    | Cr(Cp) <sub>2</sub>                 | 0.25          | 11.64                      | 5.81         | 15        |
|                     | Co(Cp) <sub>2</sub>                 | 0.25          | 11.18                      | 5.35         | 16        |
|                     | Co(CpMe) <sub>2</sub>               | 0.25          | 11.17                      | 5.34         | 17        |
|                     | Co(Cp <sup>i</sup> Pr) <sub>2</sub> | 0.15          | 11.57                      | 5.74         | 17        |
|                     | Co(Cp <sup>n</sup> Bu) <sub>2</sub> | 0.13          | 11.17                      | 5.34         | 17        |
|                     | Cr(Bz) <sub>2</sub>                 | 0.16          | 11.73                      | 5.90         | 15        |
|                     | Mo(Bz) <sub>2</sub>                 | 0.16, 0.31    | 11.64                      | 5.81         | 15, 18    |
|                     | Mo(Tol) <sub>2</sub>                | 0.13          | 11.63                      | 5.80         | 15        |
|                     | Mo(Mes) <sub>2</sub>                | 0.08, 0.15    | 11.61, 13.6                | 5.78, 7.78   | 15, 18    |
|                     | Ti(Cp)(Cot)                         | 0.23          | 12.23                      | 6.4          | 15, 19    |
|                     | Cr(Cp)(Bz)                          | 0.24          | 11.9                       | 6.07         | 15        |
|                     | Cr(Cp)(Cht)                         | 0.25          | 12.0                       | 6.17         | 15        |
|                     | Co(CpMe) <sub>2</sub>               | 0.21          | 11.59                      | 5.68         | 17        |
| 1T TaS <sub>2</sub> | Co(Cp <sup>i</sup> Pr) <sub>2</sub> | 0.17          | 12.05                      | 6.18         | 17        |
|                     | Co(Cp <sup>n</sup> Bu) <sub>2</sub> | 0.13          | 11.44                      | 5.53         | 17        |
|                     | Co(Cp) <sub>2</sub>                 | 0.25          |                            | 5.47         | 16        |
| 2H TaS <sub>2</sub> | Cr(Cp) <sub>2</sub>                 | 0.28          |                            | 5.52         | 16        |
|                     | Co(Cp) <sub>2</sub>                 | 0.42*         |                            | 5.45         | 16        |
| TaSe <sub>2</sub>   | Cr(Cp) <sub>2</sub>                 | 0.25          |                            | 5.57         | 16        |
|                     | Co(Cp) <sub>2</sub>                 | 0.2           |                            | 5.55         | 16        |
| TiS <sub>2</sub>    | Cr(Cp) <sub>2</sub>                 | 0.30          |                            | 5.55         | 16        |
|                     | Co(Cp) <sub>2</sub>                 | 0.38*         |                            | 5.52         | 16        |
| TiSe <sub>2</sub>   | Co(Cp) <sub>2</sub>                 | 0.31          |                            | 5.53         | 16        |
|                     | Cr(Cp) <sub>2</sub>                 | 0.20          |                            | 5.56         | 16        |
| NbSe <sub>2</sub>   | Co(Cp) <sub>2</sub>                 | 0.33          |                            | 5.35         | 16, 20    |
|                     | Co(Cp) <sub>2</sub>                 | 0.33          | 11.51                      | 5.38         | 21        |
| SnSe <sub>2</sub>   | Co(Cp) <sub>2</sub>                 | —             | —                          | —            | 17        |
| VSe <sub>2</sub>    | Co(Cp) <sub>2</sub>                 | —             | —                          | —            | 17        |
| HfS <sub>2</sub>    | Co(Cp) <sub>2</sub>                 | 0.38*         |                            | 5.52         | 16        |
|                     | Cr(Cp) <sub>2</sub>                 | 0.20          |                            | 5.63         | 16        |

The intercalation chemistry of the metal dichalcogenides will be reviewed in three sections, the first of which will describe the attempts of early workers to determine the guest orientation in these compounds, and the next two will contain case histories of two of the most researched and best understood of this class of intercalation chemistry and which illustrate many of the subtleties, and some of the pitfalls, encountered in this area of solid state chemistry.

### Orientation of Guest Molecules

One of the fundamental questions concerning the structure of these intercalates is the orientation of the guest molecule, and there was considerable debate in the early literature as to which of the two possible low energy orientations, depicted in Fig. 3, the metallocene molecules adopt between the host layers. The technique employed by the majority of early workers to investigate this problem was simply to consider the changes induced in both the interlayer separation and product stoichiometry for various substituted metallocene molecules and to attempt to rationalise these data in terms of the guest Van der Waals dimensions, and their consequence on both packing and interlayer distances.

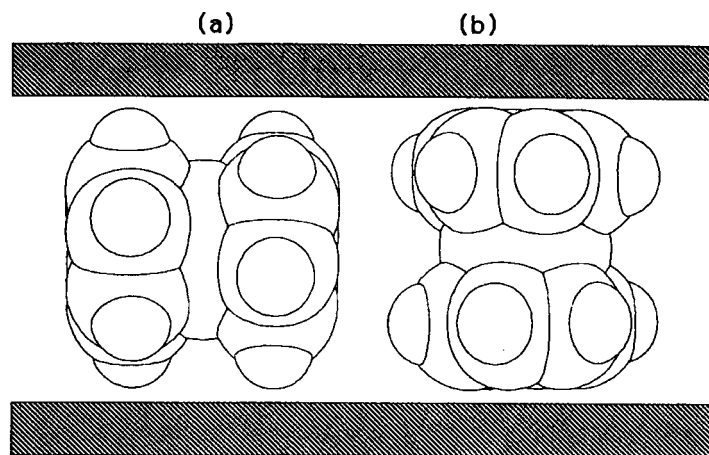


FIGURE 3 The two possible extreme orientations of a metallocene molecule in a layered host lattice. (a) the *parallel* orientation and (b) the *perpendicular* orientation.



In his original paper, Dines estimated the Van der Waals dimensions of the cobaltocene molecule to be a cylinder measuring 5.65 by 6.8 Å, and comparison of these to the observed layer expansion of ca. 5.5 Å led him to conclude that the guest molecules must adopt an orientation with their principal molecular axis parallel to the plane of the host layers (Fig. 3). Later workers, however, pointed out that the cobaltocene dimensions used by Dines were erroneous, and in particular underestimated the dimensions of the cyclopentadienyl ring.<sup>17,22</sup> In fact, as illustrated by Fig. 4, the Van der Waals surface of the cobaltocene molecule is essentially spherical, and so little can be concluded about its orientation

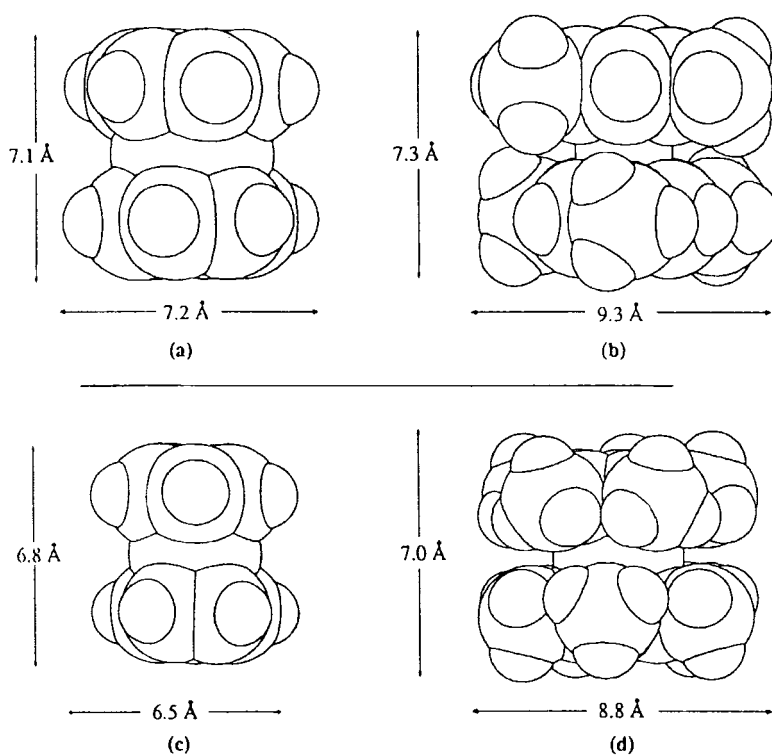


FIGURE 4 (a) Bisbenzene molybdenum, (b) bismesitylene molybdenum, (c) cobaltocene, and (d) decamethyl cobaltocene drawn using their Van der Waals dimensions to emphasize the true molecular dimensions.

from lattice expansions alone. It is clear, however, that whichever orientation the metallocene adopts, there must be either considerable compression of the guest molecule, or significant interpenetration between it and the host layers.

Interestingly, it was later pointed out<sup>23</sup> that in the crystal structure of pure cobaltocene the molecules are found to be close packed in, and have their principal axis parallel to, the {100}-plane.<sup>24</sup> The distance between these planes is found to be 5.05 Å indicating that subsequent cobaltocene layers can interpenetrate considerably and “nestle” together. This separation is close to the layer expansion found by Dines for the cobaltocene intercalates.

Despite the fact that little information can be inferred regarding guest orientation for the spherical unsubstituted metallocenes, some information can be gained by considering the effects on lattice expansion and guest occupancy as the size of the metallocene rings is altered either by the introduction of substituents or by a change in the number of ring atoms. The most complete study of this kind was published by Clement *et al.* in 1978 in a paper which reported the synthesis of 20 new metallocene intercalates.<sup>17</sup>

In the case of  $\text{ZrS}_2$  a series of intercalation compounds was synthesised in which one ring of the metallocene molecule remained a cyclopentadienyl ring, while the diameter of the second ring was systematically increased from  $\text{Cr}(\text{Cp})_2$  to  $\text{Cr}(\text{Bz})(\text{Cp})$  to  $\text{Cr}(\text{Cht})(\text{Cp})$  (Fig. 4). Along this series the interlamellar separation was found to increase from 11.44 to 11.9 to 12.0 Å, whilst the guest stoichiometry remained constant at  $0.25 \pm 0.1$ . This data was used to infer that the molecules all adopt a parallel orientation between the host layers, the gradual increase in interlamellar separation being caused by the increase in diameter of the metallocene ring system.

In contrast to this observation, for the *bis*( $\eta$ -arene) molybdenum intercalates of  $\text{ZrS}_2$  the *c*-axis was found to be essentially unchanged as the ring substitution, and hence effective ring diameter, of the guest molecule was increased from  $\text{Mo}(\text{Bz})_2$  (11.64 Å) to  $\text{Mo}(\text{Tol})_2$  (11.63 Å) to  $\text{Mo}(\text{Mes})_2$  (11.61 Å). Across this series the guest occupancy was, however, found to decrease from 0.16 to 0.13 to 0.08. The invariance of the interlamellar separation was used to infer that the guest molecules all adopt the perpendicular orientation; thus the Van der Waals dimension of the guest mol-

ecule perpendicular to the layers remains essentially constant, whereas in the plane of the layers it gradually increases, leading to a decrease in molecular packing density and the observed decrease in guest stoichiometry.

In a second study, the effect of ring substitution on the interlamellar separation of a series of cobaltocene derivatives intercalated by 1T TaS<sub>2</sub> and ZrS<sub>2</sub> was investigated. The relevant data is summarised below in Table II.

A consistent explanation of these data can be obtained by assuming that the organometallic molecules all adopt the perpendicular orientation. In the case of the branched isopropyl derivative the methyl groups will then point away from, and the hydrogens point directly towards, the host lattice layers. The effective Van der Waals length of the guest molecule along its principal axis is thus increased relative to the other two derivatives, and this would lead to the increase in interlayer separation found in both the TaS<sub>2</sub> and ZrS<sub>2</sub> intercalation compounds. This perpendicular orientation would, however, be expected to give a larger interlayer separation than the parallel orientation, but it is noted by the authors that both the Me and Bu<sup>n</sup> intercalates of ZrS<sub>2</sub> have layer expansions nearly identical to the unsubstituted derivatives (5.34, 5.34 and 5.35 Å, respectively). For the analogous TaS<sub>2</sub> compounds the Bu<sup>n</sup> and unsubstituted intercalates both have similar expansions of 5.53 and 5.47 Å, respectively, whereas that of the Me derivative is somewhat larger at 5.68 Å. In an analogous manner to that of the bis(η-ar<sup>o</sup>-ne)molybdenum intercalates the guest stoichiometry is

TABLE II

Interlamellar separation and guest occupancies of the cobaltocene intercalation compounds of TaS<sub>2</sub> and ZrS<sub>2</sub>

| Guest                               | ZrS <sub>2</sub> |                           |      | TaS <sub>2</sub> |                           |      |
|-------------------------------------|------------------|---------------------------|------|------------------|---------------------------|------|
|                                     | Stoichiometry    | Inter-lamellar Separation | Δc Å | Stoichiometry    | Inter-lamellar Separation | Δc Å |
| Co(CpMe) <sub>2</sub>               | 0.25             | 11.17                     | 5.34 | 0.21             | 11.59                     | 5.68 |
| Co(Cp <sup>i</sup> Pr) <sub>2</sub> | 0.15             | 11.57                     | 5.74 | 0.17             | 12.05                     | 6.18 |
| Co(Cp <sup>n</sup> Bu) <sub>2</sub> | 0.13             | 11.17                     | 5.34 | 0.13             | 11.44                     | 5.53 |
| Co(Cp <sup>i</sup> Bu) <sub>2</sub> | 0.00             | —                         | —    | 0.00             | —                         | —    |

observed to decrease gradually for both series of compounds. These examples show well that while some conclusions can be drawn from lattice expansions, there are clearly further subtleties involved in these compounds, and further evidence must be obtained before the guest orientation can be unambiguously invoked.

We have recently re-investigated the *bis*( $\eta$ -arene)molybdenum intercalates of zirconium disulphide using a combination of X-ray and neutron diffraction, and found the system to be considerably more complicated than was previously thought. In the case of the  $\text{ZrS}_2\{\text{Mo}(\text{Bz})_2\}_{0.31}$  a one dimensional refinement of the 001 intensities derived from both x-ray and neutron diffraction patterns indicated that the guest molecules adopt the parallel orientation between the host layers, in contradiction to the conclusions of Clement. Diffraction patterns of the bismesitylene intercalate, however, indicated the presence of two 001 series, one corresponding to an interlayer separation of 11.6 Å, as previously reported, and the other to an interlayer separation of 13.6 Å. These two separations have been tentatively assigned to the presence of *both* parallel and perpendicular orientations of the guest molecules. The relative amounts of the two species were found to be highly sensitive to both the synthetic route employed, and the sample's age and thermal history. In fact, samples could be prepared in which either completely parallel or perpendicular or a mixture of both orientations were present, and of those containing a mixture, some samples, on standing for several months, converted to totally parallel, and some to totally perpendicular containing forms.<sup>18</sup> Unpredictable behaviour of this type is an excellent illustration of some of the fascinating aspects of these materials, and has prompted the detailed investigation of several of these compounds.

#### Cobaltocene Intercalates of $\text{TaS}_2$

Clearly steric arguments alone are insufficient to determine the orientation and arrangement of the guest molecules in these systems, particularly in the case of the almost spherical unsubstituted metallocenes. In order to obtain more direct evidence as to the metallocene orientation B. G. Silbernagel, one of Dine's colleagues at Exxon Research Laboratories, performed a variable temperature solid state proton NMR study on  $\text{TaS}_2\{\text{Co}(\text{Cp})_2\}_{0.25}$ .

By studying the temperature dependence of the second moment of the cw proton line shape it is possible to infer information about both the dynamical properties of the metallocene guest, and its orientation between the host layers.

In general the line width of the proton resonance will be determined by the proton's local environment and the magnitude of both the inter and intra-molecular proton-proton dipolar interactions, which are in turn affected by the motional behaviour of the molecule. If a particular motion occurs on a time scale of ca. 10  $\mu$ s (a measure of the dipole interaction strength), the motion will result in an averaging of the dipolar interaction and usually in a reduction of its strength. This will lead to a narrowing of the proton resonance.

In the case of  $\text{TaS}_2\{\text{Co}(\text{Cp})_2\}_{0.25}$ , the resonance line shape and width was found to be largely temperature independent between 300 and 400 K, with a full width at half maximum (fwhm) of 1.5 G and a second moment ( $M_2$ ) of  $0.46 \pm 0.03 \text{ G}^2$ ; however, on cooling to 245 K the signal was found to broaden to a fwhm of 2.1 G ( $M_2 = 0.77 \pm 0.03 \text{ G}^2$ ). Subsequent cooling caused little change until around 80 K when further broadening began, with  $M_2$  reaching 4.7  $\text{G}^2$  by 10 K. The independence of  $M_2$  with temperature in the high temperature regime implies that, in contrast to the case of the ammonia intercalate  $\text{TaS}_2(\text{NH}_3)_{1.0}$ , the cobaltocene guest molecules have no translational motion on the NMR time scale at these temperatures.<sup>25</sup> Quantitative analysis of the temperature dependence of the second moment indicated that the most likely explanation for the broadenings observed was that the molecules adopt an orientation with their  $\text{C}_5$  axis parallel to the layers, and that at high temperature this axis can reorient. On cooling, however, the molecules gradually lose this motional degree of freedom, and below 245 K this mode is inactive. The onset of the second broadening at 80 K was interpreted as being due to the slowing down of the cyclopentadienyl rings, which are known to undergo rapid rotation about the metal-ring axis in metallocene molecules at room temperature.<sup>26</sup> It should, however, be pointed out that in order to perform the quantitative second moment analysis in the intermediate ( $\text{C}_5$  only) and low temperature (rigid lattice) regions, a specific model for the arrangement of the guest molecules must be assumed. The arrangement chosen was a probable, though, in

the light of later work, not necessarily unique one in which the guest molecules occupied a specific lattice invariant site between the host layers. Activation energies for the two motions were calculated to be  $34.3 \text{ kJ mol}^{-1}$  for the reorientation of the metallocene molecule and  $0.54 \text{ kJ mol}^{-1}$  for the ring rotation. This second activation energy is considerably lower than that measured for ferrocene at 80 K of  $7.5 \pm 0.8 \text{ kJ mol}^{-1}$ ,<sup>26</sup> and is a reflection of the different interactions present in the intercalation compound as compared to the pure metallocene. Clearly in the intercalate the metallocene molecule is in a much more symmetrical environment and the absence of directed bonds leads to a lowering of the activation energy.

This intercalation compound was reinvestigated in more recent years using the technique of solid state deuterium NMR.<sup>27</sup> Deuterium has a quadrupolar nucleus with spin  $I = 1$ , so the principle interactions of the nucleus with an applied magnetic field will be the Zeeman and quadrupolar interactions. The quadrupolar interaction is between the nuclear quadrupole coupling constant (NQCC) and the angularly dependent electric field gradient (efg) tensor at the nucleus, and the resultant spectrum is therefore highly sensitive to dynamical processes, and particularly to those in the region of  $10^3$ – $10^8$  Hz. In the case of metallocene molecules, for which the principal component of the static  $^2\text{H}$  efg tensor is directed along the C–D bond, rapid  $C_5$  rotation, which is known to occur in these compounds, will cause an averaging of the efg tensor, giving rise to a new tensor with an effective NQCC half that of a static deuteron, whose principal component points along the principal axis of the metallocene molecule. The principal direction of the efg tensor is thus, as pointed out by Heyes, a vector which gives direct information as to the orientation of the metallocene molecule within the layers of an intercalation compound.<sup>28</sup>  $^2\text{H}$  NMR is therefore a powerful tool for investigating the structure and dynamics of intercalation compounds.

Variable temperature solid state  $^2\text{H}$  NMR spectra were recorded on polycrystalline samples of both 2H (trigonal prismatic metal coordination) and 1T (octahedral)  $\text{TaS}_2\{\text{Co}(\eta\text{-C}_5\text{D}_5)\}_{0.25}$  between 200 and 340 K. In the case of 2H  $\text{TaS}_2\{\text{Co}(\text{Cp})\}_{0.25}$  a single Pake doublet was observed below 230 K, with a splitting of the inner discontinuities of approximately 65 KHz. This is characteristic of

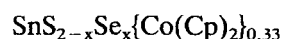
a metallocene molecule in which the cyclopentadienyl rings are undergoing rapid rotation around the  $C_5$  axis. On warming to 230 K, however, the powder line shape was observed to change, with a second inner Pake doublet growing into the spectrum, the splitting of which was approximately half that of the outer Pake doublet. This is indicative of further averaging of the efg tensor at the deuterium nucleus, and the metallocene molecules must therefore be undergoing motion in addition to the ring rotation. This motion is clearly related to that observed by Silbernagel at 245 K. Careful examination of the outer doublet revealed it to be shifted some 2000 Hz (approximately 65 ppm) up field of the outer doublet, indicating the presence of two distinct types of cobaltocene magnetic environment between the layers. This was supported by wide-line  $^{13}\text{C}$  solid state NMR studies on non-deuterated samples in which the observed line shapes could not be explained by any simple chemical shift anisotropy pattern and by  $^{13}\text{C}$  magic angle spinning spectra which seemed to indicate the presence of two environments in that the resonance observed was neither purely Lorentzian or Gaussian in shape and was interpreted as being due to the superposition of one sharp and one broad signal.<sup>29</sup>

These results were interpreted by the authors as being due to the presence of *both* extreme orientations of the guest molecules between the host layers, the exact proportions of which being highly temperature (and often sample) dependent. At low temperature only the perpendicular orientation is present, but on warming some of the guest molecules can reorient (by a process which is slow on the NMR time scale) and adopt the parallel orientation. Deuterons of these parallel molecules will be in a different magnetic environment to those of perpendicular guest molecules, hence the shift of the inner doublet relative to the outer. On further warming this parallel orientation becomes more highly populated, reaching a maximum of 30–50% (depending on both the sample and its thermal history) of the total. In addition, those molecules in the parallel orientation undergo a rotation about their  $C_2$  axis at a rate which increases in an Arrhenius fashion with temperature, for which the activation energy was estimated to be  $25.5 \text{ kJ mol}^{-1}$  (cf.  $34.3 \text{ kJ mol}^{-1}$  calculated by Silbernagel).

The spectra of  $1\text{T TaS}_2\{\text{Co}(\eta\text{-C}_5\text{D}_5)_2\}_{0.25}$  were broadly similar to those of the 2H sample in that a single Pake doublet was seen

at low temperature, and as the temperature was increased inner intensity grew into the powder line shape. For this polytype there were, however, some differences in the spectra. Firstly the shape of the inner component indicated that the metallocene molecules could undergo some motion in addition to reorientation around the  $C_2$  axis, and secondly the centre of the inner discontinuities was not shifted relative to the outer Pake doublet. These results were again interpreted as being due to the presence of solely perpendicular molecules at low temperature, with a gradual conversion of molecules into the parallel orientation as the temperature was increased, though in this case the poorer spectral resolution precluded an accurate estimate of the proportions and activation energies for the reorientation processes. The additional averaging present in the spectrum was interpreted as being due to the guest molecules not being confined to a strictly parallel orientation at higher temperatures, and their molecular axes being allowed to deviate slightly from the parallel to the plane.

The structure and dynamics of this intercalation compound are clearly much more involved than originally supposed, being dependent on both sample preparation method, host polytype and the thermal history of the sample. The paper of Silbernagel does not state the host polytype or the synthetic method used, but it is presumed to be the same as that of Dines. Also in the case of the  $2H\text{-TaS}_2\{\text{Co}(\eta\text{-C}_5\text{D}_5)\}_{0.25}$  studied by Heyes *et al.*, when one sample was re-examined after several months, the guest molecules were found to all have adopted the parallel orientation.<sup>30</sup> On cooling, however, the guest molecules realigned to adopt the perpendicular orientation. There appears to be a subtle balance in this system between the thermodynamic and kinetic factors which determine the structural preferences in these systems.



(i) *Structural Studies.* Although much research has been carried out over the last 15 years into the properties of the intercalates of the transition metal dichalcogenides, until recently almost no interest had been shown in the intercalation chemistry of non-transition-metal dichalcogenides such as  $\text{SnS}_2$  and  $\text{SnSe}_2$ . The only report of organometallic intercalation of such host lattices was the



original 1975 paper of Dines,<sup>16</sup> which reported the synthesis of  $\text{SnS}_2\{\text{Co}(\text{Cp})_2\}_{0.33}$ , and the synthesis of  $\text{SnSe}_2\{\text{Co}(\text{Cp})_2\}_{0.33}$  which was published by Benes and coworkers in 1985.<sup>21</sup> Over the past five years we have undertaken a detailed investigation of the cobaltocene intercalates of the series  $\text{SnS}_{2-x}\text{Se}_x$  using a wide variety of solid state techniques. Accounts of the crystal structure,<sup>20</sup> photoelectron spectroscopy,<sup>31</sup> electronic conductivity<sup>32</sup> and solid state deuterium NMR<sup>33</sup> have been published, such that these are now among the best understood of all metallocene intercalation compounds.

In the course of this work, we have found that it is possible to intercalate not only powdered samples of these host lattices, but also relatively large single crystals (up to approximately  $1 \text{ mm} \times 1 \text{ mm} \times 0.1 \text{ mm}$ ), and this discovery has meant that a new range of analytical techniques has become applicable to the elucidation of the detailed structure and dynamical behaviour of these materials.

Single crystals of the host materials  $\text{SnS}_{2-x}\text{Se}_x$  were grown by Iodine Vapour Phase Transport in a multizone furnace, with a linear temperature gradient of ca.  $50^\circ\text{C}$  between the load and growth end of sealed evacuated quartz ampoules. Typically 0.5 g of relatively large single crystals could be grown over a period of 14 days. Intercalation of these crystals could be achieved by heating the crystals in a concentrated toluene solution of cobaltocene without stirring (to prevent crystal damage) over a period of 5–21 days. Details of reaction times and lattice parameters are given in Table III.

TABLE III  
Reaction conditions, stoichiometries and lattice expansions for the intercalated layered materials  $\text{SnS}_{2-x}\text{Se}_x\{\text{Co}(\text{Cp})_2\}_{0.33}$

| Host Lattice                        | Temperature ( $^\circ\text{C}$ ) | Time (days) | Stoichiometry | $\Delta c$ Å |
|-------------------------------------|----------------------------------|-------------|---------------|--------------|
| $\text{SnS}_2$                      | 65                               | 5           | 0.31          | 5.46         |
| $\text{SnS}_{1.7}\text{Se}_{0.3}$   | 65                               | 7           | 0.31          | 5.24         |
| $\text{SnS}_{1.5}\text{Se}_{0.5}$   | 65                               | 9           | 0.31          | 5.20         |
| $\text{SnS}_{0.7}\text{Se}_{1.3}$   | 65                               | 14          | 0.33          | 5.26         |
| $\text{SnS}_{0.15}\text{Se}_{1.85}$ | 65                               | 17          | 0.33          | 5.50         |
| $\text{SnSe}_2$                     | 65                               | 21          | 0.33          | 5.56         |

A detailed investigation of the structure of the cobaltocene intercalate of  $\text{SnS}_2$  has been performed using a combination of both single crystal and powder X-ray and neutron diffraction, and has illustrated nicely the complementarity of the information attainable by these two techniques.<sup>20</sup>

Initial X-ray photographs indicated that these materials had a remarkably high degree of order, and a large number of hkl reflections were visible. The reflections while being sharp in  $\theta$  were, however, up to  $20^\circ$  wide in  $\Omega$ , which reflects the inherent disorder and low crystallinity of these compounds, and is indicative of a large mosaic spread being present in the crystals. For these reasons the diffraction pattern was not of sufficient quality to be recorded by conventional modern X-ray techniques, such as automated four circle diffractometry, and the diffraction pattern instead had to be recorded using the more traditional Weissenberg moving film method. In this manner it proved possible to index and obtain the intensities of a total of 177 hkl intensities and the data has allowed us to perform what we believe to be the first three dimensional structural investigation of this class of compound.

From the manner in which the data was collected and the inherent disorder of these systems, the quality of the diffraction data descended in the order  $001 > 0kl > hkl$ , and for this reason the structural refinement was performed in three stages. 001 reflections allow one to obtain structural information along the crystallographic  $c$ -axis, which in this case is the axis perpendicular to the layers. A one dimensional Fourier map of the structure was therefore calculated along this axis phased on approximate known Sn and S  $z$  coordinates. Comparison of this to maps calculated for the two possible extreme orientations of the cobaltocene guest molecule immediately suggested that  $\text{Co}(\text{Cp})_2$  adopts the parallel orientation between the host layers. We were then able to refine trial structures in which either or both extreme orientations were initially present, and, regardless of the starting model, found that the refinement converged to a model containing solely the parallel orientation, with an R factor of 13.7%.

Examination of the 0kl information allows one to calculate information about the  $bc$ -crystallographic plane. From the two-dimensional Patterson function it was immediately apparent that there is a relative shift of the host lattice layers on intercalation,

which leads to a doubling of the crystallographic  $c$ -axis. From the electron density map of Fig. 5 it can be seen that intercalation causes a shift of  $b/2$  between successive layers so that the Sn atoms no longer lie directly above one another as they do in the pristine host lattice. Presumably this is due to guest–host packing interactions, and it can be seen that the cobaltocene molecule now sits in an essentially symmetrical S environment. It is also apparent

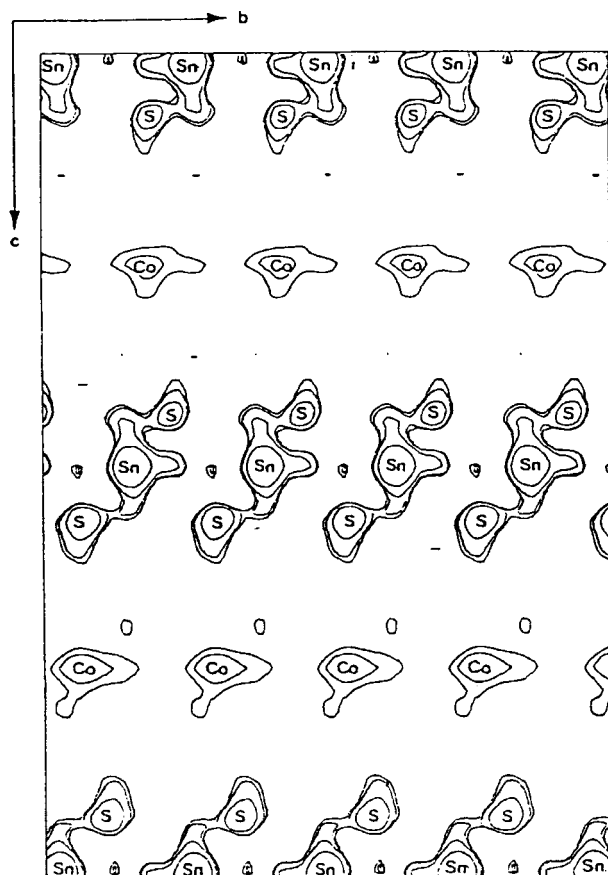


FIGURE 5 Electron density map of the  $bc$  crystallographic plane derived from the  $0kl$  Weissenberg photographs of  $\text{SnS}_2\{\text{Co}(\text{Cp})_2\}_{0.33}$  showing the  $(a/2, 0)$  layer shift that occurs on intercalation, and the specific lattice site adopted by the cobaltocene molecule.

that the cobaltocene molecule seems to adopt a specific lattice invariant site between the host layers, though the diffraction data was of insufficient quality to investigate this further.

Three dimensional refinement confirmed this layer shift and also indicated that there was a lattice shift in the  $a$  as well as the  $b$  direction, though the paucity of experimental data prevented further structural refinement.

In order to obtain structural information about this intercalation compound over and above that attainable by X-ray diffraction a neutron diffraction experiment was undertaken. Neutron diffraction should be a powerful tool for examining in particular the behaviour of the guest molecules in these systems. In an X-ray diffraction experiment, where electrons are responsible for the scattering, only 19% of the total scattering is due to the guest molecules, whereas in a neutron diffraction experiment using a deuterated sample of  $\text{SnS}_2\{\text{Co}(\eta\text{-C}_5\text{D}_5)_2\}_{0.33}$ , the relatively large coherent scattering of C and D mean that as much as 44% of the total scattering is caused by the guest molecules.

Initially it was decided to record the diffraction pattern of an aligned sample of single crystals of  $\text{SnS}_2\{\text{Co}(\eta\text{-C}_5\text{D}_5)_2\}_{0.33}$  so as to collect just the 001 reflections and perform a one dimensional refinement. Such a refinement is extremely sensitive to the guest orientation, and the results of the X-ray study were confirmed in that the cobaltocene molecule was shown to adopt solely the parallel orientation.

Further studies on a powdered sample of this intercalation compound showed several reflections which could not be indexed simply upon a  $\text{SnS}_2$  lattice with an expanded  $c$ -axis. Simple packing considerations show that a cobaltocene molecule is too large to fit inside each unit cell of the host compound, which leads to the fractional guest occupancy observed. Thus, if there is a specific low energy lattice site that the guest molecule adopts between the host lattice layers, as indicated by the two dimensional X-ray refinement, a superlattice is expected, and it is this superlattice which gives rise to the extra Bragg reflections observed. Preliminary studies on the related compound  $\text{ZrS}_2\{\text{Co}(\eta\text{-C}_5\text{D}_5)_2\}_{0.25}$  indicate a similar phenomenon in this system. Further work, including a single crystal neutron diffraction experiment is in progress.

The orientation and dynamical behaviour of the guest molecule

was also investigated using solid state  $^2\text{H}$  NMR. In the case of a single axially symmetric C–D bond one expects to see a doublet in the  $^2\text{H}$  NMR spectrum, the splitting of which reflects both the angle relative to the field and the motional behaviour of the C–D bond in question. Thus  $^2\text{H}$  NMR is, as discussed above, a potentially excellent probe of molecular motion in the solid state and for metallocene intercalates a single crystal  $^2\text{H}$  NMR experiment can be used to investigate both the orientation and the motional behaviour of the guest molecule. The exact details of the single crystal experiment required are discussed below, and summarised in Fig. 6 for clarity.

If the guest molecules adopted the perpendicular orientation between the host lattice layers, then with the field applied perpendicular to the host lattice layers, one would expect to see a doublet with a separation of  $3/4$  of the Nuclear Quadrupole Coupling Constant (NQCC), or approximately 140 kHz for the case of an aromatic C–D bond. If the guest molecule adopted the parallel orientation, however,  $\text{C}_5$  ring rotation, which has been observed down to very low temperatures in these systems,<sup>34</sup> would cause a further averaging of the electric field gradient tensor at the deuterium nucleus and a consequent reduction in the doublet separation by a factor of half to ca. 70 kHz. These splittings would be independent of the rate of molecular reorientation about the  $\text{C}_2$  axis.

If, however, the field is applied parallel to the host lattice layers, then the rate of  $\text{C}_2$  motion can be probed. For the parallel guest orientation, if the molecules rotate in the fast regime on the  $^2\text{H}$  NMR time scale ( $>10^8$  kHz) then  $\text{C}_2$  rotation leads to a further reduction of the doublet splitting to ca. 35 kHz. If, however, the molecules were static, with a random orientation of their principal axis to the  $ab$ -plane, then a powder pattern would be expected. Between these two extremes of motion complex line shapes would be expected.

The experimental spectra obtained are shown in Fig. 7. It can be seen that with the  $ab$  plane oriented perpendicular to the applied field a single doublet is obtained of separation 68 kHz. Similar spectra were observed for a large number of single crystals, and no evidence for a double separation of 136 kHz was ever seen. This indicates that the crystals adopt solely the parallel orientation

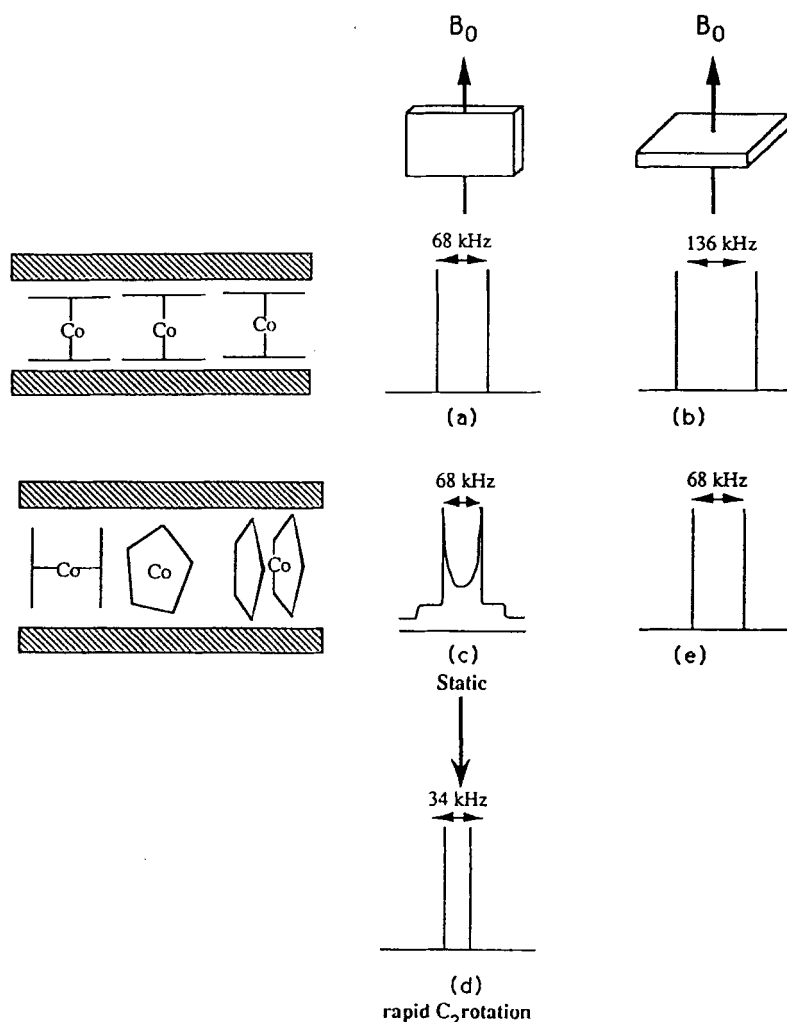


FIGURE 6 Single crystal  $^2\text{H}$  NMR spectra expected for aligned single crystals of a metallocene intercalation compound. If the molecules adopt the perpendicular orientation, one expects (a) a doublet of separation ca. 68 kHz with the field applied parallel to and (b) 136 kHz with the field applied perpendicular to the host layers. If the guest molecules adopt the parallel orientation, one expects (c) a powder spectrum if the molecules are static on the  $^2\text{H}$  NMR timescale and (d) a doublet of separation ca. 34 kHz if the molecules undergo rapid  $C_2$  reorientation with the field parallel to the layer planes, and (e) a doublet of separation ca. 68 kHz with the field perpendicular to the host layers.

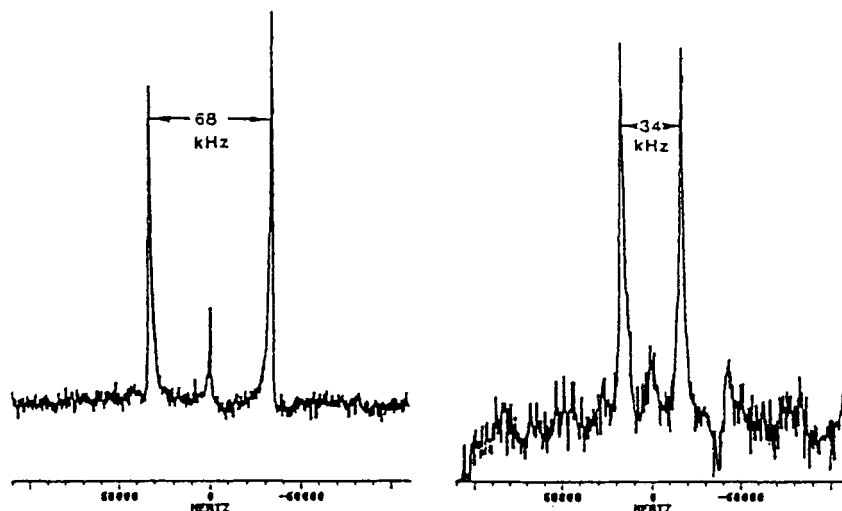


FIGURE 7 Single crystal  $^2\text{H}$  NMR of  $\text{SnS}_2(\text{Co}(\text{Cp})_2)_{0.33}$  with the field (a) perpendicular and (b) parallel to the host lattice layers.

between the host layers, which supports both the X-ray and neutron diffraction results.

A typical spectrum with the field oriented parallel to the layers is shown in Fig. 7b. The splitting of 34 kHz implies that the molecules are undergoing rapid reorientation around their  $\text{C}_2$  axis at this temperature. Spectra from other crystals, however, showed broader line shapes, the doublet only being clearly resolved at higher temperatures. It therefore seems likely that there is a distribution of rates of rotation in this system at room temperature, with different crystals exhibiting slightly different behaviour. The exact form of the spectrum was also found to be dependent on the sample's thermal history.

(ii) *Electronic Properties.* This system is also of considerable interest because of the remarkable changes in the conductivity properties of the host lattices which occur on intercalation, which are largely due to charge transfer from the guest molecules to the host lattice layers, and the resulting mixed valency. The electronic properties of this series of compounds were initially studied using a combination of X-ray and UV Photoelectron Spectroscopy. X-ray

Photoelectron Spectroscopy shows that the main Sn, S and Se emission peaks remain essentially unchanged on intercalation. For Sn 4d emission, however, the intercalated compounds show a second peak at lower binding energy than the main host emission peak. The proportion of this reduced tin species is approximately 10–12% of the total and this, together with  $^{119}\text{Sn}$  Mössbauer evidence, suggests that the reduced species is Sn(II) rather than Sn(III). On examination of the Co( $2P_{3/2}$ ) and C(1s) emissions, two separate signals are resolvable, suggesting the presence of two unique organometallic species between the layers. Comparison of these spectra to those of pure, unoxidised  $\text{Co}(\text{Cp})_2$  and the oxidised species  $[\text{Co}(\text{Cp})_2]^+[\text{PF}_6]^-$  suggests that the cobaltocene molecules are present between the layers in both oxidised and unoxidised form, in approximate ratio 2:1, the exact figure being dependent on the host selenium content. This is in contrast to the classically held view that guest ionisation is a prerequisite for, and occurs simultaneously to, the process of intercalation. This observation is further supported by both EPR measurements, where the existence of a metal based radical is observed, and magnetic studies in which  $\text{SnS}_2\{\text{Co}(\text{Cp})_2\}_{0.33}$  was found to be paramagnetic, obeying the Curie–Weiss law between 4 K and 300 K with values of  $\theta = -9.17$  K and  $\mu_{\text{eff}} = 0.12 \mu_{\text{B}}$ . This moment, although small, corresponds to approximately 25% of the guest molecules being present in unoxidised paramagnetic form. This is in contrast to magnetic measurements on  $\text{TaS}_2\{\text{Co}(\text{Cp})_2\}_{0.25}$  in which the molar magnetic susceptibility was found to be  $+88 \times 10^{-6} \text{ emu mol}^{-1}$ , somewhat lower than that of pure  $\text{TaS}_2$ ,<sup>35</sup> and temperature independent between 2 and 300 K, suggesting a complete ionisation of the guest molecules on intercalation.

This partial charge transfer from the guest molecules to the host layers gives rise to the remarkable conductivity properties of the  $\text{SnS}_{2-x}\text{Se}_x\{\text{Co}(\text{Cp})_2\}_{0.33}$  series, and these properties have been recently reviewed.<sup>36</sup> We have synthesised a series of compounds ranging from  $x = 0$  to  $x = 2.0$ , and measured the variation of conductivity with temperature for both the host lattices and their intercalation compounds. The sulphur-rich intercalation compounds ( $x \leq 1.3$ ) exhibit a classical Arrhenius type semiconducting behaviour, and the activation energy is found to decrease steadily from 0.45 eV to 0.09 eV as the selenium content is increased. The



selenium-rich members of the series ( $x = 1.8$  and  $2.0$ ) are, however, best described as extremely low activation energy semiconductors in that they exhibit metallic like behaviour above about 150 K (where the carrier mobility term becomes important relative to the carrier concentration) and semiconducting behaviour below this temperature.

On intercalation of cobaltocene, with the concomitant partial electron transfer from the guest molecules to the host layers, the conductivity of these systems is found to alter dramatically. Figure 8 shows the variation in conductivity with temperature for the whole series of compounds.

The sulphur-rich intercalation compounds ( $x \leq 1.3$ ) are found to be semiconducting. Interestingly the conductivity (which is found to be higher than that of the pristine host for  $x = 0$ , yet slightly lower for the other three members of the series) is found to be essentially three dimensional in nature, giving a good fit to an  $\exp(T_0/T)^{1/4}$  dependence.<sup>37</sup>

This three dimensionality is surprising in view of the inherent two dimensionality of these layered materials, but can be rationalised in light of the XPS data, and the evidence it gives for mixed valency in these compounds. The conductivity of these compounds is best interpreted in terms of an impurity band model, which suggests that hopping of electrons between the mixed valence cobaltocene guest and host layers would occur. This hopping, which will clearly reduce the anisotropy of the conductivity, is presumably the source of the three dimensionality.

The selenium-rich members of the series ( $x = 1.8, 2.0$ ) exhibit a more remarkable change in conductivity on intercalation in that they become metallic conductors at all temperatures. The impurity band presumably now overlaps the conduction band to some extent, which gives rise to the metallic behaviour.

On cooling, both compounds are found to exhibit a metal-superconducting transition, at 5.7 and 8.3 K, respectively, and the diselenide intercalate has the highest known superconducting critical temperature ( $T_c$ ) of any layered chalcogenide or intercalation compound. Low dimensional materials of this kind are of extreme interest in the study of superconductivity, as early models of superconductivity suggested that the off diagonal long range order (ODLRO) associated with the superconducting state could not be

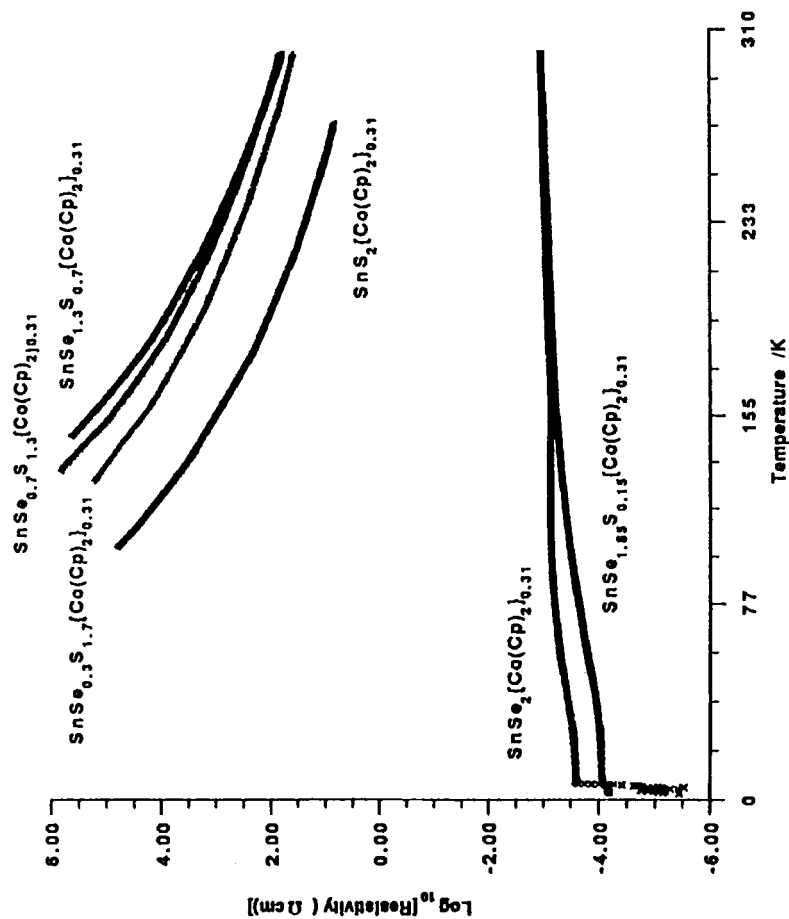


FIGURE 8 Plot of  $\log_{10}[\text{resistivity } (\Omega\text{cm})]$  vs. temperature (K) for single crystals of the intercalation compounds  $\text{SnS}_{2-x}\text{Se}_x\{\text{Co}(\text{Cp})_2\}_{0.33}$  where  $0 \leq x \leq 2$ .

established in mathematically one and two dimensional systems. Studies on layered intercalated materials also allow one to investigate the importance, and dependencies, of interlayer Josephson coupling on the mechanism of superconductivity.

We have therefore studied the anisotropy of the superconductivity in these compounds by measurement of the critical fields  $H_{c1}$  and  $H_{c2}$  perpendicular and parallel to the host layers by orienting single crystals of the diselenide intercalate within a SQUID magnetometer. The Ginzburg–Landau coherence lengths derived from this critical field data have shown that  $\text{SnSe}_2\{\text{Co}(\text{Cp})_2\}_{0.33}$  exhibits an almost isotropic superconductivity. This observation is in sharp contrast to that found in other superconducting host lattices such as  $\text{NbSe}_2$ ,  $\text{TaS}_2$  and  $\text{TaS}_{1.6}\text{Se}_{0.4}$ , but is in agreement with earlier studies of superconductivity in  $\text{TaS}_2\{\text{Co}(\text{Cp})_2\}_{0.32}$ .<sup>35</sup> Presumably the origins of this three dimensionality lie once again in the mixed valency of the guest layer which would be expected to facilitate interlayer conduction and thus reduce the electronic anisotropy, but would, as a region containing paramagnetic molecules, be expected to act as a superconducting pair breaking medium. The existence of this interlayer conduction mechanism is presumably also the reason why the superconducting critical temperature of these compounds is higher than that found in other layered compounds. It would obviously be of extreme interest to investigate the effect of introducing a different metallocene molecule into the interlamellar region, to see how this would affect the superconducting properties of these compounds. Unfortunately, attempts to intercalate other organometallic guests such as  $\text{Cr}(\text{Cp})_2$ ,  $\text{Fe}(\text{Cp})_2$ ,  $\text{Ni}(\text{Cp})_2$  and  $\text{Co}(\text{Cp}^*)_2$  have so far proved unsuccessful.

### 3. INTERCALATION INTO $\text{MPS}_3$ HOSTS

The transition metal hexachalcogenohypodiphosphates,  $\text{MPS}_3$ , were first reported by Friedel in 1894, and extensively studied in the late 1960's and early 1970's by Hahn and Klinge.<sup>38</sup> They form a series of layered structures which are, to a first approximation, very similar to the layered metal dichalcogenides. Thus their structure can be described as two dimensional  $\text{MX}_2$  layers of the  $\text{CdCl}_2$  type in which one third of the cations have been substituted by  $\text{P}_2$

pairs so that the metal ions and P—P pairs are approximately octahedrally coordinated by the S atoms, which are themselves arranged in a distorted cubic close packed lattice. The stacking of these layers most commonly gives rise to a monoclinic unit cell with space group  $C2/m$  with typical unit cell parameters, those of the first characterised  $\text{FePS}_3$ , of  $a = 5.93 \text{ \AA}$ ,  $b = 10.28 \text{ \AA}$ ,  $c = 6.722 \text{ \AA}$  and  $\beta = 107.16^\circ$ , through rhombohedral forms are also known. Figure 9 shows two views of the structure.

An alternative, and perhaps more informative picture of the structure in light of its unusual intercalation chemistry, is to view it not as a classical close packed structure, but in terms of an array

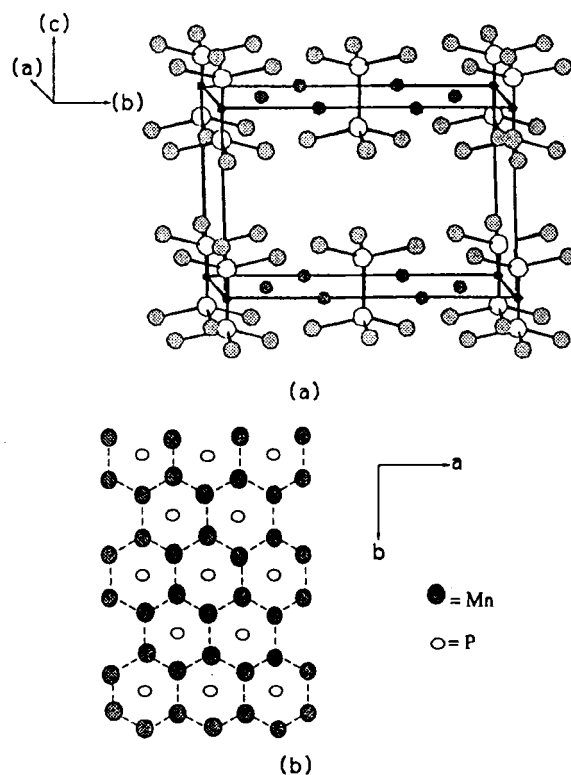


FIGURE 9 The layered structure of  $\text{MnPS}_3$ , emphasising (a) the  $\text{P}_2\text{S}_6$  groups by omitting the Mn—S bonds and (b) the honeycomb like nature of the  $ab$  plane. In (b) Sulphur atoms are omitted for clarity.

of  $M^{2+}$  cations which are coordinated to  $P_2S_6^{4-}$  bridging ligands so as to form two dimensional slabs of formula  $M_2P_2S_6$ . This model is supported by the fact that the  $P_2S_6^{4-}$  entity is well known and characterised both in aqueous solution and as simple ionic compounds such as  $Na_4P_2S_6$ . Further support comes from the fact that these materials can be precipitated in an amorphous form from such aqueous solutions simply by addition of the transition metal ion to a solution of  $Na_4P_2S_6$  in methanol or acetonitrile.<sup>17,39</sup>

A large number of metal phosphorous chalcogenides have been synthesised,<sup>40</sup> and their structures<sup>41</sup> and physical properties<sup>42</sup> are well known.

In view of the similarity of these compounds to the well known transition metal dichalcogenides, they were initially considered as merely an exotic extension of this class of compound, and early work on their intercalation chemistry followed the development of that of the metal dichalcogenides. Thus  $MPS_3$  compounds were shown to react with electron donating species such as  $Bu^+Li$  and  $Co(Cp)_2$  and to intercalate Lewis bases such as amines and pyridine.<sup>43</sup> The first indication that these compounds exhibit a chemistry which is unique to this particular lattice, and one of the most unusual reactions of intercalation chemistry, came in 1980 when Clement reported that the  $MnPS_3$  lattice would react spontaneously with aqueous solutions of ionic salts  $G^+X^-$  (where  $G$  can range from simple ionic species such as  $K^+$  and  $NH_4^+$  to species as large as, for example,  $Ru(bipy)_3^{2+}$  to give compounds of general formula  $Mn_{1-x}PS_3[G]_{2x}(H_2O)_y$ . In these compounds charge balance has been maintained by the loss of one  $Mn^{2+}$  ion from the *intralayer* region for every two  $G^+$  ions that are adopted in the interlayer region.<sup>44</sup> This chemistry means that intercalation reactions are no longer restricted to a few electron rich organometallic compounds, and almost any sandwich compound which forms an alcohol or water stable cationic species can be intercalated either directly or via preintercalation of a smaller readily exchangeable species such as  $K^+$ . Sandwich compounds which have been intercalated by both direct and ion exchange methods are summarised in Tables IV and V.

This reaction pathway is most facile for the host lattices which contain  $d^5$  and  $d^{10}$  ions ( $Mn$ ,  $Cd$ ,  $Zn$ ), where the crystal field stabilisation is low, but can be extended under slightly more rig-

TABLE IV  
Sandwich intercalation compounds of  $MPX_3$  lattices prepared by direct insertion

| Host Lattice | Guest        | Stoichiometry | c Spacing Å | $\Delta c$ Å | Reference |
|--------------|--------------|---------------|-------------|--------------|-----------|
| $MnPS_3$     | $Co(Cp)_2$   | 0.33          | 11.79       | 5.29         | 45        |
|              | $Cr(Bz)_2$   | 0.24          | 12.42       | 5.92         | 45        |
|              | $Fe(Cp)(Bz)$ | 0.30          | 12.05       | 5.55         | 45        |
| $CdPS_3$     | $Fe(Cp)_2$   | not given     | not given   | not given    | 46        |
|              | $Co(Cp)_2$   | 0.36          | 11.84       | 5.32         | 47        |
|              | $Cr(Bz)_2$   | high Cr       | not given   | not given    | 47        |
| $FePS_3$     | $Co(Cp)_2$   | 0.39          | 11.74       | 5.32         | 48        |
|              | $Cr(Bz)_2$   | 0.32          | 12.38       | 5.96         | 45        |
| $NiPS_3$     | $Co(Cp)_2$   |               | 11.68       | 5.33         | 48        |
| $ZnPS_3$     | $Co(Cp)_2$   | 0.28          | 11.74       | 5.31         | 45        |
|              | $Cr(Bz)_2$   | 0.33†         | 12.35       | 5.8          | 49        |

†Indicates a high chromium analysis.

orous conditions (reflux in the presence of a reagent such as EDTA to complex the departing host metal ions) to hosts such as  $FePS_3$  and  $NiPS_3$ . Interestingly the ease of this chemistry has also been related to the thermal parameters of the transition metal ion as determined by their crystal structure.<sup>53</sup> The labile  $Mn^{2+}$  ion is found to have relatively high thermal parameters, and can be thought of as almost “rattling” in a somewhat loose cage of sulphur atoms. This cation exchange chemistry clearly requires a remarkable degree of structural flexibility of the host lattice, and this flexibility is also shown by the existence of compounds such as  $V_{0.78}PS_3$ ,<sup>54</sup>  $In_{2/3}PS_3$ <sup>55</sup> and  $Mn_{1-x}Cu_{2x}PS_3$ ,<sup>56</sup> all of which contain metal deficient layers.

#### Structure and Magnetic Properties of $Mn_{0.83}PS_3\{Co(Cp)_2\}_{0.34}(H_2O)_{0.3}$

One of the most remarkable features of the intercalation chemistry of these host lattices is the dramatic changes seen in the magnetic behaviour upon intercalation.  $MnPS_3$  is best described as a two dimensional Heisenberg antiferromagnet, and has a Neel temperature,  $T_N$ , of 78 K. Neutron diffraction studies have determined the magnetic structure, which consists of a two dimensional honeycomb lattice in which each  $Mn^{2+}$  ion is antiferromagnetically cou-

TABLE V  
Sandwich intercalation compounds of MPX<sub>3</sub> lattices prepared by ion exchange

| Host              | Guest   | x     | c Å   | Δc Å | Formula   | Reference |
|-------------------|---|-------|-------|------|---|-----------|
| MnPS <sub>3</sub> | [Co(Cp) <sub>2</sub> ] <sup>+</sup> I <sup>-</sup>                      | 0.33  | 11.82 | 5.32 | Mn <sub>0.83</sub> PS <sub>3</sub> [Co(Cp) <sub>2</sub> ] <sub>0.33</sub> (H <sub>2</sub> O) <sub>0.3</sub>   | 44        |
|                   | [Cr(Bz) <sub>2</sub> ] <sup>+</sup> I <sup>-</sup>                      | 0.33  | 12.26 | 5.76 | Mn <sub>0.83</sub> PS <sub>3</sub> [Co(Cp) <sub>2</sub> ] <sub>0.33</sub> (H <sub>2</sub> O) <sub>0.3</sub>   | 44        |
|                   | [Fe(Cp)(Bz)] <sup>+</sup> [PF <sub>6</sub> ] <sup>-</sup>               | 0.30  | 12.05 | 5.55 | Mn <sub>0.83</sub> PS <sub>3</sub> [Fe(Cp)(Bz)] <sub>0.20</sub> (H <sub>2</sub> O) <sub>y</sub>   | 45        |
|                   | [Fe(Cp)(C <sub>6</sub> Me <sub>6</sub> )] <sup>+</sup>                  | 0.28  | 13.5  |      | Cd <sub>0.62</sub> PS <sub>3</sub> [Fe(Cp)(C <sub>6</sub> Me <sub>6</sub> )] <sub>0.28</sub>  | 50        |
|                   | [Ru(Cp)(p-cymene)] <sup>+</sup>   | 0.21  | 12.2  |      | Na <sub>0.18</sub> K <sub>0.01</sub> (H <sub>2</sub> O)<br>Mn <sub>0.71</sub> PS <sub>3</sub> [Ru(Cp)(p-cymene)] <sub>0.21</sub>  | 50        |
| CdPS <sub>3</sub> | [Fe(Cp)(o-C <sub>6</sub> H <sub>4</sub> Cl <sub>2</sub> )] <sup>+</sup> | 0.4   | 12.6  |      | Na <sub>0.37</sub> K <sub>0.01</sub> (H <sub>2</sub> O)<br>Mn <sub>0.8</sub> PS <sub>3</sub> [Fe(Cp)(o-C <sub>6</sub> H <sub>4</sub> Cl <sub>2</sub> )] <sub>0.4</sub> K <sub>0.02</sub> (H <sub>2</sub> O) | 50        |
|                   | [Ru(Cp*)(C <sub>6</sub> H <sub>6</sub> )] <sup>+</sup>                  | 0.25  | 13.6  |      | Mn <sub>0.87</sub> PS <sub>3</sub> [Ru(Cp*)(C <sub>6</sub> H <sub>6</sub> )] <sub>0.25</sub> K <sub>0.01</sub>  | 50        |
|                   | [Co(Cp) <sub>2</sub> ] <sup>+</sup> I <sup>-</sup>                      | 0.34  | 11.84 | 5.32 | Cd <sub>0.84</sub> PS <sub>3</sub> [Co(Cp) <sub>2</sub> ] <sub>0.32</sub> (solV) <sub>0.3</sub>   | 51        |
|                   | [Fe(Cp)(C <sub>6</sub> Me <sub>6</sub> )] <sup>+</sup>                  | 0.28  | 13.5  |      | Cd <sub>0.62</sub> PS <sub>3</sub> [Fe(Cp)(C <sub>6</sub> Me <sub>6</sub> )] <sub>0.28</sub> Na <sub>0.18</sub> K <sub>0.01</sub> (H <sub>2</sub> O)  | 50        |
|                   | [Co(Cp) <sub>2</sub> ] <sup>+</sup> I <sup>-</sup>                      | 0.34  |       | 5.32 | Fe <sub>0.83</sub> PS <sub>3</sub> [Co(Cp) <sub>2</sub> ] <sub>0.34</sub> (H <sub>2</sub> O) <sub>0.3</sub>   | 51        |
| NiPS <sub>3</sub> | [Co(Cp) <sub>2</sub> ] <sup>+</sup> I <sup>-</sup>                      | 0.36  | 11.9  |      | NiP <sub>0.90</sub> S <sub>3</sub> [Co(Cp) <sub>2</sub> ] <sub>0.36</sub> Na <sub>0.03</sub> (H <sub>2</sub> O) <sub>0.5</sub>  | 51        |
| ZnPS <sub>3</sub> | [Co(Cp) <sub>2</sub> ] <sup>+</sup> Cl <sup>-</sup>                     | 0.3   | 12.4  |      | NiP <sub>0.92</sub> S <sub>3</sub> [Cr(Bz) <sub>2</sub> ] <sub>0.30</sub> Na <sub>0.09</sub> (H <sub>2</sub> O) <sub>0.7</sub>  | 52        |
|                   | [Co(Cp) <sub>2</sub> ] <sup>+</sup> I <sup>-</sup>                      | 0.28  | 11.72 | 5.29 | Zn <sub>0.86</sub> PS <sub>3</sub> [Co(Cp) <sub>2</sub> ] <sub>0.28</sub> (H <sub>2</sub> O) <sub>y</sub>   | 45        |
|                   | [Cr(Bz) <sub>2</sub> ] <sup>+</sup> I <sup>-</sup>                      | 0.21* | 12.25 | 5.82 | Zn <sub>0.9</sub> PS <sub>3</sub> [Co(Cp) <sub>2</sub> ] <sub>0.21</sub> (H <sub>2</sub> O) <sub>y</sub>  | 45        |
|                   | [Fe(Cp)(Bz)] <sup>+</sup> [PF <sub>6</sub> ] <sup>-</sup>               | 0.20* | 12.08 | 5.65 | Zn <sub>0.9</sub> PS <sub>3</sub> [Fe(Cp)(Bz)] <sub>0.20</sub> (H <sub>2</sub> O) <sub>y</sub>  | 45        |
|                   | [Fe(Cp)(C <sub>6</sub> Me <sub>6</sub> )] <sup>+</sup>                  | 0.42  | *     |      | Zn <sub>0.78</sub> PS <sub>3</sub> [Fe(Cp)(C <sub>6</sub> Me <sub>6</sub> )] <sub>0.42</sub> (H <sub>2</sub> O) <sub>2.0</sub>  | 50        |

\*Indicates sample amorphous to X-rays.

pled to its three nearest in-plane neighbours, and in which all the spins point in a direction perpendicular to the layer plane.<sup>57</sup> The effects of intercalation on the magnetic properties of the lattice are shown by Fig. 10. At high temperatures the intercalation compound is paramagnetic, with antiferromagnetic interactions which are weaker than those in the pristine host, and obeys the Curie–Weiss law. On cooling to approximately 40 K a steep increase in the susceptibility is observed, and below these temperatures the susceptibility is large and essentially constant. In fact, the material displays a spontaneous magnetisation in zero applied field below this temperature. Zero field ac susceptibility measurements have shown the Curie temperature,  $T_c$ , to be 33 K.<sup>58</sup> Thus the process of intercalation has transformed the antiferromagnetic host into a ferro or ferrimagnetic intercalation compound.

The origins of this bulk magnetism are still not fully understood. The saturation value of the magnetisation of  $3980 \text{ emu G mol}^{-1}$  of Mn is only a fraction (ca. 1/6th) of the saturation value of  $27,900 \text{ emu G mol}^{-1}$  expected for full alignment of  $\text{Mn}^{2+}$  ( $S = 5/2$ ;  $M_{\text{sat}} = N\mu_{\text{B}}gS$ ) ions. Examination of other intercalation compounds synthesised by the ion exchange route indicated that the value of  $T_c$  depended on the number of Mn vacancies,  $x$ , presumably due to spin dilution effects, yet the value of the susceptibility,  $\chi$ , was largely independent of  $x$ . For example, room temperature susceptibilities of the  $\text{NH}_4$  intercalate ( $x = 0.2$ ) and the *n*-octyl  $\text{NH}_3$  intercalate ( $x = 0.11$ ) were found to be very similar.<sup>58</sup> Also it was found that the magnetic properties of  $\text{MnPS}_3\{\text{Co}(\text{Cp})_2\}_{0.34}$  prepared by the standard direct reduction mechanism from a dry toluene solution of cobaltocene, in which there was presumed to be no loss of intralayer  $\text{Mn}^{2+}$ , exhibited almost identical magnetic behaviour to the ion exchange prepared intercalate.

The magnetic behaviour was therefore interpreted as being due to spin canting in the sample. The antiferromagnetic interactions in the host lattice are essentially due to a super-exchange mechanism involving the Mn–S–Mn bridges, and are as such extremely sensitive to Mn–S bond angles and distances, which could be slightly affected on intercalation. This spin canting could arise from either anti-symmetric exchange, although this is generally small for Mn(II) ions, or from single ion anisotropy energies which can cause canting



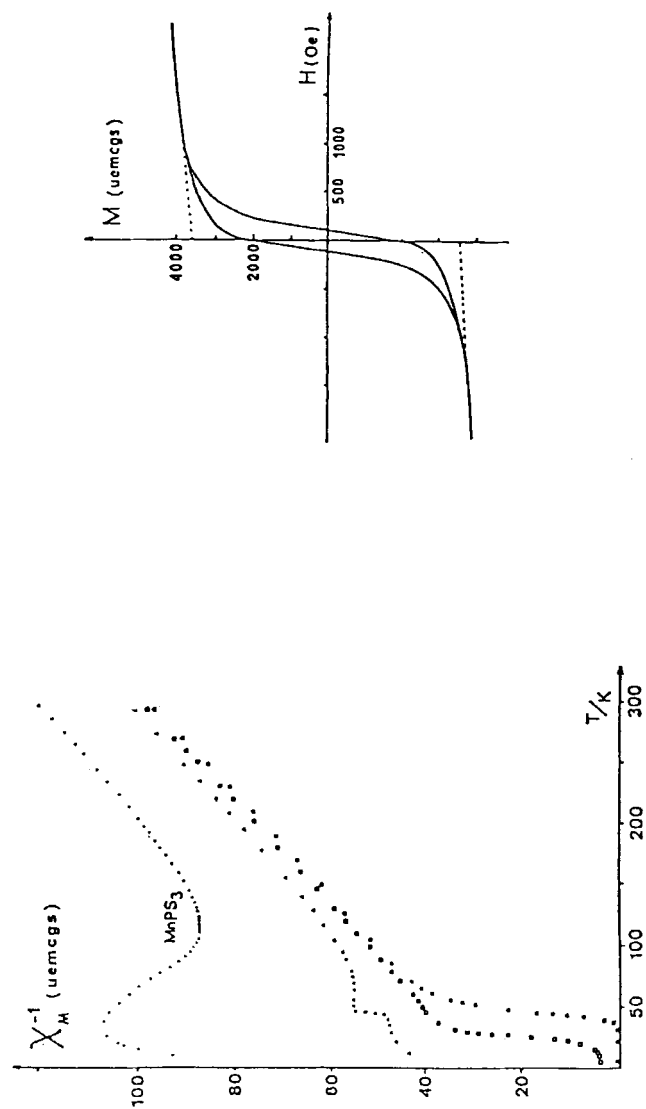


FIGURE 10 (a) Temperature dependence of the reciprocal susceptibility of  $\text{MnPS}_3$  (●) and its intercalates  $\text{Mn}_{1-x}\text{PS}_3\text{G}_x(\text{H}_2\text{O})_2$ ; (▲)  $G = \text{methyltris (octyl) ammonium}^+$ , (□)  $G = \text{NH}_4^+$ , (■)  $G = \text{Co}(\text{Cp})_2^+$ . (b) Magnetisation (per mole of manganese) at 4.2 K for  $G = \text{Co}(\text{Cp})_2^+$  showing a hysteresis loop typical of a weak ferromagnet. After Clement (Ref. 58).

if the crystal field axes of neighbouring ions are not parallel; however, this is also expected to be a weak effect for Mn(II).

In the absence of a complete structural analysis of the intercalation compound it is impossible to be more precise about the exact source of the magnetism. For this reason EXAFS was employed to probe the changes in local environment around the manganese ion caused by intercalation, and to see if the magnetism could be rationalised on this basis.

Thus variable temperature EXAFS studies were performed on the pristine host and both the direct and ion exchange intercalation compounds. Both intercalation compounds showed a significant increase in disorder of the Mn environment on intercalation, and a very slight increase in the mean square deviation of all distances around the Mn, indicating a slight change in the manganese local environment on intercalation.

That these changes in the manganese environment are closely related to the magnetic properties of this material is beyond doubt, and was further verified by Michalowicz *et al.* in a combined EXAFS and magnetic study on a range of closely related intercalation compounds.<sup>59</sup> The difficulty now lies in rationalising the fact that both the direct and ion exchange intercalation compounds exhibit identical magnetic behaviour, a fact which is also found in the related compounds  $\text{FePS}_3\{\text{Co}(\text{Cp})_2\}_{0.37}$  and  $\text{Fe}_{0.83}\text{PS}_3\{\text{Co}(\text{Cp})_2\}_{0.34}$ .<sup>58</sup> This phenomenon, coupled with the fact that the EXAFS spectra of both compounds are very similar, seems to indicate that *both* reaction pathways involve loss of manganese from the host lattice layers. This loss of intralayer manganese would at first seem unlikely to occur in a non-aqueous medium, but if the host structure is viewed, as discussed above, as a polynuclear coordination compound rather than a classical metal sulphide, then the familiarity of ligand exchange and redox reactions in organic solvents lends some support to the mechanism.

It therefore seems likely that many of the conclusions drawn in the early literature on these intercalation compounds could be reinterpreted in light of this exchange mechanism, which seems to be a general feature of the chemistry of these host lattices. In particular, there has been much discussion concerning the fate of the electrons which, in a classical description, are passed from the guest molecules to the host lattice on intercalation. The conduc-

tivities of these host lattices are not generally found to change dramatically on intercalation, and so the electrons are presumed to be localised in the structure. As yet there has been no convincing evidence, and many possibilities suggested, for their location.<sup>46,48,60-62</sup> The ultimate fate of any ions leaving the intralamellar region in direct insertion reactions remains, however, equally unclear. Elemental analysis indicates that they do not leave the bulk of the structure, and one obvious possibility is that they reside, along with the guest molecules, in the interlamellar region. There is no direct evidence for this location, but the existence of metal atoms in such sites has also been suggested for the non-stoichiometric compounds formed between  $\text{Cr}(\text{Bz})_2$  and  $\text{FePS}_3$ .<sup>63</sup>

Further investigations of the magnetic structure of these compounds are currently being performed by comparing the neutron diffraction patterns of these compounds above and below their Curie temperatures. Preliminary results suggest that the direction of the spin vector lies perpendicular to the plane of the host lattice layers, which would seem to contradict the model of the weak ferromagnetism being due to a canting of the spins. An alternative interpretation of the magnetism could therefore be that the creation of manganese vacancies in the layers leads to an imbalance in the two spin sublattices, and thus gives rise to a net bulk ferromagnetism. Interestingly in this particular case the number of vacancies of approximately 1/6th ties in nicely with the value of the net magnetism which is approximately 1/6th of that expected for a parallel arrangement of  $\text{Mn}^{2+}$  ions. Further work, including magnetic and diffraction studies on single crystals of these intercalation compounds, is in progress.

While the magnetic behaviour of these compounds is clearly largely a property of the host layers, the magnetism will be affected by the presence of the guest molecules. The behaviour of these molecules has been investigated by a number of techniques including diffraction, infra-red spectroscopy and  $^2\text{H}$  solid state NMR. In one of the first papers to give direct evidence of the orientation of a metallocene molecule in a layered lattice Mathey *et al.* performed variable temperature infra-red and Raman spectroscopy on both powdered and single crystal samples of  $\text{Mn}_{0.83}\text{PS}_3\cdot\{\text{Co}(\text{Cp})_2\}_{0.34}(\text{H}_2\text{O})_y$ .<sup>64</sup> From this study they were able to determine a number of properties of the guest molecule. Firstly band in-

tensities in the polarised infra-red spectra of platelets of  $\text{Mn}_{0.83}\text{PS}_3\{\text{Co}(\text{Cp})_2\}_{0.34}(\text{H}_2\text{O})_y$  indicated that the molecules adopt an orientation with their principal axis parallel to the host layer, and secondly the temperature dependence of the position and width of the  $68\text{ cm}^{-1}$  peak in the Raman spectrum, a band which is assigned to an external cation mode, suggested that the metallocene molecule rotates around its  $\text{C}_2$  axis at room temperature, with a correlation time of the order of  $10^{-11}\text{ s}$ . These conclusions were verified in a second inelastic neutron scattering study.<sup>65</sup> There were also a number of interesting differences observed between the host and intercalated lattice spectra, and in particular the appearance of several strong low frequency absorptions was interpreted in terms of the formation of a unit cell of increased multiplicity on intercalation. This is indicative of the formation of a superlattice which could be due to either an ordering of the Mn vacancies or an ordering of the  $\text{Co}(\text{Cp})_2$  guest molecules. This superlattice has more recently been observed in the X-ray and neutron diffraction spectra of both this and other related intercalation compounds. Work on this is still in progress. Preliminary single crystal and powdered  $^2\text{H}$  NMR spectra of this compound have supported the IR conclusions that the guest molecules adopt the parallel orientation, though analysis of these spectra is complicated by the presence of paramagnetic  $\text{Mn}(\text{II})$  ions in the lattice, and is again still in progress.

#### Cobaltocene Intercalates of $\text{CdPS}_3$

The synthesis of the closely related intercalation compounds of  $\text{CdPS}_3$  and  $\text{Co}(\text{Cp})_2$  was first reported in 1980 by Audiere.<sup>47</sup> The  $\text{CdPS}_3$  lattice was found to undergo a very similar chemistry to  $\text{MnPS}_3$  in that intercalation could be achieved either in toluene solution at  $110^\circ\text{C}$  or via an ion exchange method using an ethanolic solution of cobaltocenium iodide. Initial studies showed that the ion exchange mechanism is less efficient in  $\text{CdPS}_3$  than  $\text{MnPS}_3$ , so that higher temperatures and longer reaction times are required for full intercalation. Reaction rates can, however, be significantly increased by performing the reactions under conditions in which the cadmium ions are complexed as they leave the host lattice.

Typical conditions using buffered EDTA at pH 10 lead to rapid intercalation at room temperature.

Infra-red spectra of these compounds indicated that the guest molecules were present in their oxidised form between the layers in both the Mn and Cd compounds, and subsequent variable temperature Raman and infra-red experiments led the authors to conclude that the guest molecules again adopt the parallel orientation between the layers, and are motionally disordered at room temperature.<sup>49,64</sup>

The orientation and dynamics of the guest molecule and the electronic properties of the system have also been examined by Cleary and co-workers.<sup>66,67</sup> In an initial study single crystals of  $\text{CdPS}_3\{\text{Co}(\text{Cp})_2\}_{0.39}$  were synthesised in two steps, initial preintercalation of the host by pyridine followed by exchange of pyridine for  $\text{Co}(\text{Cp})_2$ . ESR spectra at 113 K of these crystals indicated the presence of neutral cobaltocene between the layers, which is in contradiction to the infra-red results of Audiere, although it should be remembered that Audiere's experiments were all performed on polycrystalline samples. Optical absorbance measurements suggested that >80% of the cobaltocene was present in its neutral, unoxidised form.

Since the ESR spectrum obtained from a neutral cobaltocene molecule is highly anisotropic, ESR is potentially an excellent probe for determining the orientation of such paramagnetic guest molecules in these layered host lattices. By performing ESR measurements on aligned single crystals of  $\text{CdPS}_3\{\text{Co}(\text{Cp})_2\}_{0.39}$  Cleary *et al.* concluded that at 113 K the  $\text{Co}(\text{Cp})_2$  molecules adopt the perpendicular orientation, which is again in contradiction to that suggested previously.

In a second, quantitative, study on this system performed in 1990, the amount of unoxidised  $\text{Co}(\text{Cp})_2$  was revised to  $17 \pm 3\%$  of the total, which is close to the value found for  $\text{Co}(\text{Cp})_2$  in  $\text{SnS}_2$ .<sup>68</sup> In this study the samples were prepared by direct insertion of the guest molecule at  $180 \pm 5^\circ\text{C}$ . Variable temperature studies on aligned samples again suggested that the molecules adopt the perpendicular orientation at low temperature, though it should be remembered that ESR is now only sensitive to 17% of the molecules. On warming the signal was found to disappear around 150 K, so the high temperature structure could not be investigated.

Subsequent cooling caused the signal to reappear, but the exact appearance of the spectrum was slightly changed on each cooling cycle. This was interpreted as being due to a freezing out of the motion of guest molecules between the layers, the exact structure of the low temperature form being disordered in a different manner each time. The authors also stated that the molecules could be reorienting between the layers at high temperatures, in a manner analogous to that described by Heyes for  $\text{TaS}_2\{\text{Co}(\text{Cp})_2\}_{0.26}$ , such that at room temperature up to 50% of the molecules are in the parallel orientation.

In order to investigate the differences between their results and those of earlier researchers the FTIR spectrum of the sample was recorded. The large crystals used in the ESR study were, however, found to be inhomogeneous, being transparent in some regions and opaque in others such that the infra-red spectrum could only be recorded in the transparent regions. In these regions no evidence of unoxidised  $\text{Co}(\text{Cp})_2$  could be found, and all the bands observed could be assigned to cobaltocenium species. Low temperature spectra, in temperature regions where the ESR observations were made, were not, however, reported.

In an extremely interesting second set of experiments ESR spectra were recorded on a powdered sample of the intercalation compound to compare more directly these results to those of Audiere. When the 7 K spectrum was recorded 1 hour after work-up neutral cobaltocene was again observed in the sample. After 24 hours, however, the ESR signal had disappeared despite the fact that the sample had remained isolated in a sealed, air tight, sample holder throughout.

This result has two important ramifications. Firstly it suggests that powdered host lattices can behave in an inherently different manner to single crystals, and that differences in reactivity are not merely related to surface area. This increased oxidising power of the lattice relative to that of single crystals was related by the authors to the higher concentration of surface imperfections in the powdered sample, and the effect that such imperfections have on oxidising power, as shown by work on electron injection into related layered dichalcogenide semiconductors. Secondly this result implies that the process of guest oxidation can occur *after* intercalation has occurred. For these host lattices, where the possibility

of cations leaving the intralamellar region is important, this will have important consequences regarding the fate of the expelled metals, since they clearly can't leave the intercalated lattice once work-up is complete, and all solvent has been removed from the system.

In conclusion, it seems that in these host lattices there is an extremely subtle balance of properties in that ions will migrate out of the host lattice only in polar aqueous media where they are favourably complexed by the solvent, but when such interactions are not possible prefer to remain, presumably coordinated in some manner to sulphur atoms, within the intercalation compound.

#### 4. FeOCl INTERCALATION CHEMISTRY

The metal oxyhalides were among the first layered inorganic host lattices to display intercalation chemistry, and it was shown in the 1960's that the FeOCl and AlOCl lattices could react with gaseous or liquid ammonia to form intercalation compounds such as FeOCl.NH<sub>3</sub>, though these compounds will often react further via substitution of the Cl atom giving rise to species such as FeONH<sub>2</sub>.<sup>69,70</sup> One of the most readily apparent features of the chemistry of FeOCl, which has been the most widely studied of these host lattices, is its oxidising power, and it has been shown that FeOCl will intercalate molecules with a  $pK_a$  of 2.8 and above.<sup>71</sup> This oxidising power is demonstrated by the fact that until recently FeOCl was the only host lattice that would directly intercalate ferrocene. FeOCl also has the ability to intercalate a variety of electron donors such as tetrathiafulvalene (TTF) and perylene (PE), forming an extremely interesting series of low dimensional mixed valence compounds, and to perform in situ oxidative polymerisation of guest molecules such as pyrrole which forms highly conducting polymers.<sup>72-77</sup>

A wide range of metallocene molecules have been intercalated in FeOCl and are summarised in Table VI.

The synthesis of iron oxychloride was first reported over a hundred years ago, although its layered structure was not described until 1934 and fully refined until 1967.<sup>81-83</sup> The structure, which is shown in Fig. 11, is best described as being made up of distorted cis-(Fe<sub>2</sub>Cl<sub>2</sub>O<sub>4</sub>) octahedra which share half their edges to produce a

TABLE VI  
Sandwich intercalation compounds of FeOCl

| Host Lattice | Guest  | Stoichiometry | c Spacing    | $\Delta b$ | Reference |
|--------------|--|---------------|--------------|------------|-----------|
| FeOCl        | Cr(Cp) <sub>2</sub>                          | 0.14          | 13.10        | 5.19       | 22        |
|              | Fe(Cp) <sub>2</sub>                          | 0.16, 0.13    | 13.10        | 5.19       | 22        |
|              | Fe(CpMe) <sub>2</sub>                        | 0.09          | 13.1         | 5.19       | 78        |
|              | Fe(Cp*) <sub>2</sub>                         | 0.06, 0.07    | 15.0         | 7.09       | 79        |
|              | Fe(CpMe <sub>4</sub> Et) <sub>2</sub>        | –             | 15.46        | 7.55       | 78        |
|              | Fe(Cp)(CpCHO)<br>(0.055 glyme)               | 0.09          | 13.1         | 5.19       | 78        |
|              | Fe(Cp)(CpCO <sub>2</sub> H)<br>(0.056 glyme) | 0.14          | 12.9         | 4.89       | 78        |
|              | Co(Cp) <sub>2</sub>                          | 0.18, 0.16    | 13.10, 12.85 | 5.19, 4.94 | 22, 23    |
|              | Ru(Cp) <sub>2</sub> (0.064 glyme)            | 0.01          | 13.00        | 5.09       | 78        |
|              | Ru(Cp) <sub>2</sub> (0.12 glyme)             | 0.02          | 13.0         | 5.09       | 78        |
| TiOCl        | Co(Cp) <sub>2</sub>                          | –             | 12.78        | 4.86       | 80        |
| VOCl         | Co(Cp) <sub>2</sub>                          | –             | 13.16        | 5.12       | 80        |

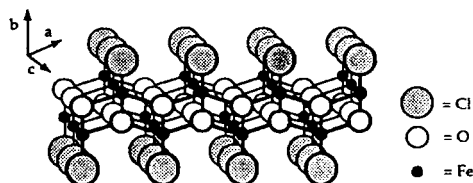


FIGURE 11 The layered structure of FeOCl.

central layer of (FeO)<sub>n</sub>, with chlorine atoms protruding from both sides of this sheet. FeOCl crystallises in the orthorhombic space group, Pmnm, and has unit cell parameters  $a = 3.7729$ ,  $b = 7.9104$ ,  $c = 3.3026$ . A large number of MOX lattices have been synthesised and their unit cells have been accurately refined and reported.<sup>84</sup> This study also related the ease of intercalation of these lattices to the thermal coefficient in the direction perpendicular to the slabs. Thus FeOCl, which has the largest thermal parameter, has by far the most facile intercalation chemistry.

Despite the large number of sandwich intercalates prepared, it is the ferrocene intercalates that have received the bulk of the



attention as regards their detailed structural and electronic properties, and these will now be discussed in more detail.

#### Intercalation of Ferrocene and Its Derivatives into FeOCl

The intercalation of ferrocene into FeOCl was first described by Halbert and Scanlon in 1979, and was quickly followed by reports of other metallocene intercalates.<sup>22,23,85</sup> It was quickly discovered that the exact nature and stoichiometry of the compounds produced is highly dependent on the precise reaction conditions. Thus the temperatures required for intercalation are found to be highly dependent on the choice of solvent, occurring at room temperature in glyme, as compared to 80–100°C in toluene, and in some cases solvent co-intercalation is observed.<sup>78</sup> It was also found that Fe(Cp)<sub>2</sub> could be intercalated directly from the gas phase. The exact reaction temperature is also found to be critical in that at higher temperatures (>60°C) decomposition is frequently observed, giving rise to side products such as chlorinated guest species and  $\alpha$ -Fe<sub>2</sub>O<sub>3</sub>.<sup>85,86</sup>

Early studies on these compounds revealed that they possessed a remarkable degree of crystallinity, and the powder patterns of the intercalates were found to index on an orthorhombic cell with *a* and *c* cell constants essentially unchanged from the pristine host, but with *b* both greatly expanded and doubled. Systematic absences in the powder pattern indicated that the cell was body centred cubic. These cell parameters and absences were later confirmed by Laue and Weissenberg single crystal photographs.<sup>87</sup>

These crystallographic results can be easily and convincingly rationalised if the guest molecules are assumed to adopt the parallel orientation between the host layers and to penetrate into the Cl layer to a certain extent. The packing of successive host layers is then optimised by a translation of alternate layers of (1/2, 0, 1/2) such that the cobaltocene molecules adopt a symmetrical lattice site. This process, which will clearly lead to a doubling of the crystallographic *b*-axis, is illustrated schematically in Fig. 12. Similar shifts are observed in other FeOCl intercalation compounds, and have, for example, been shown to occur in the formation of FeOCl(TTF)<sub>0.12</sub>, whose structure was refined by time of flight neu-

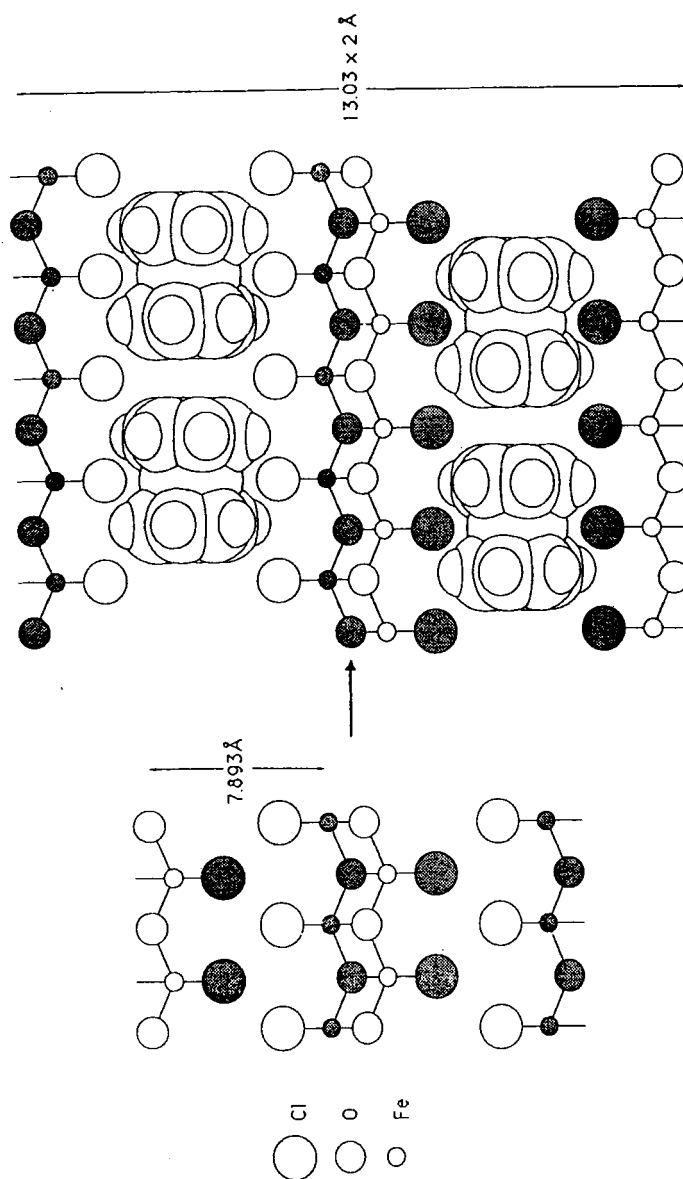


FIGURE 12 The layer shifts that occur on intercalation of  $\text{Fe}(\text{Cp})_2$  into  $\text{FeOCl}$ . Unshaded atoms are at  $z = 0$  and shaded at  $z = 1/2$ . After Palvadeau (Ref. 87).

tron diffraction, and is among the best understood of all molecular intercalates.<sup>72</sup>

There are several pieces of evidence to support this assumption of the parallel orientation. Firstly the authors have compared the observed lattice expansion of 5.14 Å to the crystal structure of cobaltocene itself in which, as discussed above, the molecules are found to be arranged in close packed planes with the “parallel” orientation, and an interplanar separation of 5.05 Å. Secondly, the larger layer expansions observed for the substituted ferrocene  $\text{Fe}(\text{C}_5\text{Me}_4\text{Et})_2$  of 7.55 Å and  $\text{Fe}(\text{Cp}^*)_2$  of 7.1 Å were found to be closely related to the additional steric bulk of the molecules.<sup>22,80</sup>

There was some controversy in the early literature of these compounds as to the fate of the electrons which were presumed to have been transferred from the guest molecule to the host layers on intercalation. Initial studies by Halbert *et al.* indicated that there was no significant enhancement in the conductivity of the  $\text{FeOCl}$  intercalates; they all appear to behave as thermally activated semiconductors.<sup>80</sup> Mössbauer studies by Stahl, however, indicated that the electrons were highly mobile within the layers, and at least  $10^4$  times more so than in  $\text{FeOCl}$ . These apparent inconsistencies were therefore investigated in a thorough two part investigation of the physical properties of this compound by Palvadeau and co-workers using a combination of Mössbauer, diffraction and conductivity techniques.<sup>87,88</sup>

Variable temperature Mössbauer studies showed that this compound exhibits a gradual change in properties as the temperature is lowered.<sup>87</sup> At room temperature the Mössbauer spectrum showed no peak due to either  $\text{Fe}^{2+}$  in the host lattice, or due to the  $[\text{Fe}(\text{Cp})_2]^+$  intercalated guest molecule, despite the presumed guest oxidation and host reduction on intercalation. From this it was concluded that at these elevated temperatures electron hopping, which is fast on the Mössbauer time scale, must be occurring, and that there was therefore only partial charge transfer from the guest to the host occurring. As the temperature was lowered (between 300 and 100 K), however, it became possible to distinguish both the  $\text{Fe}^{2+}$  reduced sites in the lattice and a signal due to the ferrocenium ion, indicating that the electrons become localised within the layers at these temperatures. The relative intensities of the host  $\text{Fe}^{2+}$  and ferrocenium guest signals indicated that guest–host

charge transfer was complete. As the temperature was lowered further, the compound was found to undergo an antiferromagnetic transition with a Neel temperature,  $T_N$ , estimated to be 75 K. That this is lower than the Neel temperature of the pristine host ( $T_N = 92$  K) is presumably due to the substitution of  $\text{Fe}^{3+}$  ( $S = 5/2$ ) ions by  $\text{Fe}^{2+}$  ( $S = 2$ ), and the consequent spin dilution.

These conclusions concerning the electronic behaviour were confirmed by a series of conductivity measurements on single crystals of  $\text{FeOCl}$  and  $\text{FeOCl}\{\text{Fe}(\text{Cp})_2\}_{0.17}$ .<sup>88</sup> The pristine host was found to be an activated semiconductor between 200 and 300 K, with an anisotropy as indicated by the relative conductivities parallel and perpendicular to the layer planes of  $\sigma_{\parallel}/\sigma_{\perp} = 100$ . On intercalation, however, the conductivity was found to increase dramatically, and activation energies for conduction fell to  $Ea_{\parallel} = 0.08$  eV and  $Ea_{\perp} = 0.13$  eV (as compared to 0.25 eV and 0.34 eV for the pristine host). Interestingly the anisotropy of the conductivity was found to remain essentially unchanged, despite an increase of the interlamellar separation of some 5 Å.

The authors were therefore able to conclude that the conductivity in these systems is caused by electron hopping between  $\text{Fe}^{2+}$  and  $\text{Fe}^{3+}$  sites, the conductivity of the host being due to trace  $\text{Fe}^{2+}$  impurities, and the considerable enhancement of the conductivity on intercalation being caused by the formation of additional  $\text{Fe}^{2+}$  sites due to guest–host electron transfer. The lack of any significant change in the anisotropy of conductivity on intercalation can be explained in light of the Mössbauer evidence, which indicates that the guest molecules can become involved in the mixed valency of the system and again, as in the case of the cobaltocene intercalates of the tin dichalcogenides, act as an interlayer coupling mechanism.

## 5. INTERCALATION CHEMISTRY OF OXIDE, PHOSPHATE AND HYDROGEN PHOSPHATE LATTICES

The intercalation of simple organometallic sandwich compounds into a number of layered oxide, phosphate and hydrogen phosphate lattices has also been reported. Detailed structural and physical studies on these compounds have so far been fairly limited, and so their intercalation chemistry will be discussed only briefly.

The intercalates successfully prepared, and the observed lattice expansions, are summarised in Table VII.

#### Intercalates of $V_2O_5$

The structure of  $V_2O_5$  is most easily thought of as being derived from that of  $ReO_3$  by the shearing of two  $ReO_3$  chains. It is thus made up of a mixture of edge and vertex sharing octahedra, though it should be pointed out that the structure is considerably distorted from this idealised model and the vanadium coordination is actually closer to square pyramidal than octahedral. This gives rise to a layered structure illustrated schematically by Fig. 13. There are, however, weak vanadium–oxygen bonds between the layers, and  $V_2O_5$  consequently behaves much more like a three dimensional framework than the lattices previously considered, and intercalation is limited to small ions such as  $Li^+$  and  $Mg^{2+}$ .<sup>96</sup> Early reports that  $V_2O_5$  could intercalate cobaltocene<sup>17</sup> were not reproduced by later workers,<sup>89</sup> and lattice decomposition, presumably via a reductive process, was probably being observed.

$V_2O_5$  layers can, however, be conveniently prepared via the sol-gel method from the polymerisation of decavanadic acid. The materials so produced are not only of extreme interest for their enhanced conductivity, reactivity and anti-static properties relative to single crystals of  $V_2O_5$ , but because their method of synthesis gives them an inherent processibility and, for example, means that they can be easily grown as thin films. The detailed structure of these materials is too involved for this review, and the interested reader is referred elsewhere.<sup>97–100</sup> but can be thought of as consisting of  $V_2O_5$  like regions some 27 Å by 3.6 Å which are linked together by water molecules to form anisotropic ribbons up to 10 nm wide and 10 μm long, giving rise to compounds of formula  $V_2O_5 \cdot nH_2O$  in which the value of  $n$  is highly dependent on reaction conditions and temperature. These hydrated gels have been shown to readily undergo intercalation reactions, which are thought to proceed principally via proton exchange, and the intercalation of cobaltocenium and ferrocenium ions has been reported.<sup>89,101</sup> From the observed lattice expansions of 4.4 Å both the cations were presumed to adopt the parallel orientation.

Recent syntheses by our group include the intercalation of the

TABLE VII

Sandwich intercalation compounds of the layered oxides, phosphates and hydrogen phosphates.  $\Delta c$  has been used to indicate the increase in interlayer separation, as in previous tables, though it should be pointed out that some of these host lattices are usually indexed on cells with  $b$  as the interlayer axis

| Host Lattice  | Guest                    | Stoichiometry | $c$ Å    | $\Delta c$ Å | Reference |
|---|--------------------------|---------------|----------|--------------|-----------|
| $V_2O_5$  | $Fe(Cp)_2$               | 0.4           | 13.2     | 4.4          | 89        |
|   | $Fe(Cp^*)_2$             |               | 15.4     | 6.6          | 90        |
|   | $Co(Cp)_2$               |               | 13.2     | 4.4          | 89        |
|   | $Co(Cp^*)_2$             |               | 13.2     |              | 90        |
| $\alpha\text{-VOPO}_4 \cdot H_2O \cdot EtOH$                                | $Fe(Cp)_2$               | 0.11, 0.35    | 8.5, 9.9 | 4.4, 5.8     | 91, 92    |
|   | $Fe(CpMe)_2$             |               | 10.3     | 6.2          | 92        |
|   | $Fe(Cp)(CpEt)$           |               | 8.8      | 4.7          | 92        |
|   | $Fe(Cp)(Cp^iBu)$         |               | 8.8      | 4.7          | 92        |
|   | $Fe(Cp)(CpCH_2OH)$       |               | 10.0     | 5.9          | 92        |
|   | $Fe(Cp)(CpCH_2CH_2OH)$   |               | 10.0     | 5.9          | 92        |
| $\alpha\text{-VOPO}_4$<br>$\alpha\text{-Zr(HPO}_4)_2 \cdot 2H_2O$           | $Co(Cp)_2$               | 0.52          | 10.1     | 6.0          | 92        |
|   | $Fe(Cp)_2$               |               | 9.65     | 5.4          | 93        |
|   | $Co(Cp)_2$               |               |          | 4.4          | 94        |
|   | $Fe(Cp)(CpCH_2CH_2NH_2)$ |               |          | 14.54        | 95        |
| $\alpha\text{-Sn(HPO}_4)_2 \cdot H_2O$<br>$HU_2PO_4 \cdot 2H_2O$<br>$MoO_3$ | $Fe(Cp)(CpCH_2NMe_2)$    | 0.81          | 20.7     | 12.9         | 91        |
|   | $Co(Cp)_2$               |               |          |              | 94        |
|   | $Fe(Cp)(CpCH_2CH_2NH_2)$ |               |          | 13.2         | 95        |

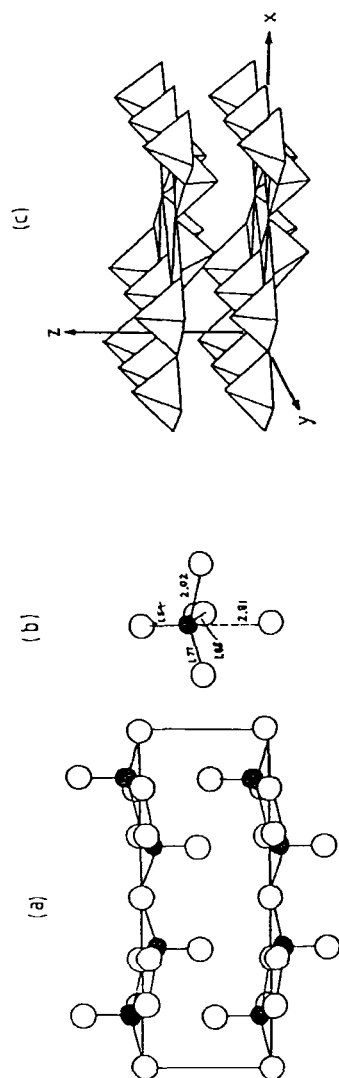


FIGURE 13 The structure of  $V_2O_5$ , emphasising (a) the layered nature of the structure, (b) the extreme nature of the distortion of the  $VO_6$  octahedra and (c) how the structure is best visualized in terms of edge sharing  $VO_6$  square pyramids (after A. M. Chippendale).

non-spherical decamethylferrocenium and decamethylcobaltocenium ions, which give rise to interlamellar separations of 15.4 and 13.2 Å ( $\Delta c = 6.6$  Å and 4.4 Å), respectively. The fact that the lattice expansion on intercalation of the ferrocenium, cobaltocenium and decamethyl cobaltocenium ions are all identical might instead suggest that all these guests adopt the perpendicular orientation, whereas the larger expansion observed for the decamethyl ferrocene is due to its adoption of the parallel orientation. Clearly more information is required to determine unambiguously the orientation of the guest molecule, and factors such as the effect of interlamellar water and co-intercalated solvent will also have to be taken into account.

#### Intercalates of $\alpha$ -VOPO<sub>4</sub>

The layered structure of  $\alpha$ -VOPO<sub>4</sub> was first reported by Jordan and Calvo in 1973.<sup>102</sup> The structure can be described as being made up of distorted VO<sub>6</sub> octahedra which share four oxygen vertices with four different PO<sub>4</sub> tetrahedra in the *ab* plane (the layer plane). The remaining two trans oxygens are then corner shared between octahedra in adjacent layers. The nature of the distortion of the VO<sub>6</sub> octahedra is such that there is one long (2.857) and one short (1.580) V–O distance perpendicular to the layer planes. The short bond length is characteristic of a V=O group, while the long bond, being greater than the sum of the Van der Waals radii, is expected to be weak. A more informative view of the structure is therefore to consider it as consisting of layers of VO<sub>5</sub> square pyramids, which are linked by the coordination of an apical oxygen of one square pyramid to the vacant coordination site of another in an adjacent layer.<sup>103</sup>

This weak interlayer bonding makes  $\alpha$ -VOPO<sub>4</sub> and related compounds excellent candidates for intercalation chemistry, and two extreme types of reaction have been observed. With Lewis bases such as water, alcohols, amines and pyridines the driving force for intercalation is the completion of the vanadium coordination sphere by the guest molecule. Thus in, for example, the case of pyridine intercalation, the weak interlayer oxygen–vanadium bond is broken, and nitrogen becomes coordinated to the base of the VO<sub>5</sub> square pyramid. The second type of intercalation, which is of more



relevance to this article, involves charge transfer from the guest molecules to the host lattice, giving rise to partial reduction of V(V) to V(IV), and in this way a number of metallocene molecules have been intercalated (Table VII). Thus Matsubayashi and co-workers successfully intercalated  $\text{Fe}(\text{Cp})_2$ , and a number of its derivatives, and  $\text{Co}(\text{Cp})_2$  into  $\text{VOPO}_4 \cdot \text{H}_2\text{O} \cdot \text{EtOH}$ .<sup>92,104</sup> A combination of ESR and XPS spectroscopic measurements confirmed that intercalation was accompanied by an oxidation of the guest and reduction of the host lattice. Interesting trends in the lattice expansion were observed, with ferrocene and its methyl, methoxy and ethoxy derivatives giving an initial increase in intralamellar separation of ca. 6.0 Å, whereas the Et and Bu<sup>n</sup> derivatives gave expansions of only 4.7 Å. The authors concluded, though the Van der Waals parameters they used were those incorrectly given by Dines in 1975, that the larger d spacings corresponded to metallocenes in the perpendicular orientation and the smaller to those in the parallel orientation.

Interestingly, after approximately 30 days the expansions of the intercalates of ferrocene and its methyl derivative were found to decrease to 4.7 Å, and this was interpreted by the authors as being due to a reorientation of the cation to the presumed more stable parallel form.

The presence of solvent molecules, which can coordinate to the host layer, is obviously an important, and potentially complicating, factor in the intercalation chemistry of these lattices. To eliminate such complications Davidson *et al.* have recently intercalated anhydrous  $\text{VOPO}_4$  with ferrocene directly from the gas phase.<sup>93</sup> The compounds so produced exhibited different stoichiometry ( $x = 0.22$ ) and interlamellar expansions (5.34 Å) to those prepared via solution methods, but again indicated that an electron transfer from ferrocene to the host layer occurs on intercalation.

### Intercalates of $\text{MoO}_3$

The crystal structure of  $\text{MoO}_3$  was first described independently by Bräkken and Wooster in 1931, and a more detailed structural refinement was reported by Kihlberg in 1963.<sup>105–107</sup> The structure, which is drawn schematically in Fig. 14, can be described as containing zig-zag chains of edge sharing distorted  $\text{MoO}_6$  octahedra

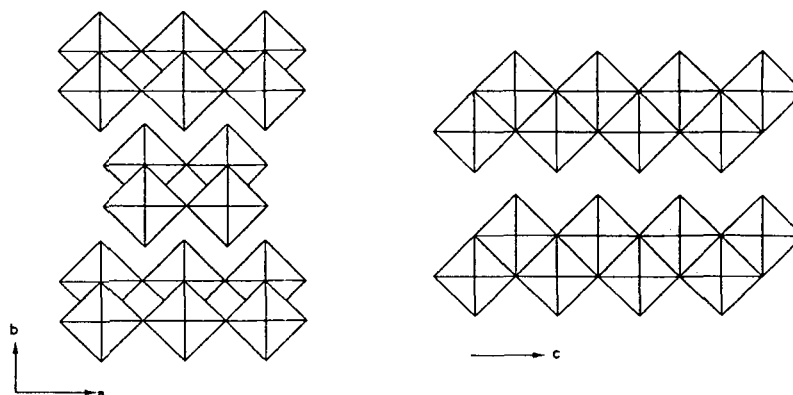


FIGURE 14 The structure of  $\text{MoO}_3$ .

which are linked together by corner sharing. The structure, unlike that of  $\text{V}_2\text{O}_5$ , therefore contains a true Van der Waals gap, and would be expected to exhibit a wide range of intercalation reactions.

Reports of organometallic intercalation compounds into  $\text{MoO}_3$  have, however, been extremely limited. In 1978 Clement *et al.* reported seeing a change in the diffraction pattern on exposure to toluene solutions of cobaltocene,<sup>17</sup> but there have been no further reports of this in the literature. More recently functionalised derivatives, such as 2-aminoethyl ferrocene have been successfully intercalated and their properties probed by a combination of diffraction,  $^{57}\text{Fe}$  Mössbauer, PES and  $^2\text{H}$  solid state nmr measurements.<sup>95,108</sup>

#### References

1. C. Schafhäütl, J. Prakt. Chem. **21**, 15 (1841).
2. K. Fredenhagen and G. Cadenbach, Z. Anorg. Allg. Chem. **158**, 249 (1926).
3. W. R. Rüdorff and H. H. Sick, Angew. Chem. **3** (1959).
4. M. S. Whittingham and A. J. Jacobson, *Intercalation Chemistry* (Academic Press, New York, 1982), p. 697.
5. R. Schöllhorn, Intercalation Compounds, in *Inclusion Compounds*, eds. J. L. Atwood, J. E. D. Davies and D. D. MacNicol (Academic Press, 1982), p. 249.
6. R. H. Friend and A. D. Yoffe, Adv. Phys. **36**, 1–94 (1987).

7. F. Levy, Intercalation Chemistry, in *Physics of Layered Compounds* (Riedel, Dordrecht, 1979).
8. D. O'Hare, in *Inorganic Materials*, eds. D. W. Bruce and D. O'Hare (J. Wiley & Sons, London, 1992).
9. F. R. Gamble, F. J. DiSalvo, R. A. Klemm and T. H. Geballe, *Science* **168**, 568–70 (1970).
10. F. R. Gamble, J. H. Osiecki, M. Cais, R. Pisharody, F. J. DiSalvo and T. H. Geballe, *Science* **174**, 493–7 (1971).
11. F. J. DiSalvo, R. Schwall, T. H. Gamble and J. H. Osiecki, *Phys. Rev. Lett.* **27**, 310–313 (1971).
12. D. E. Prober, R. Schwall and M. R. Beadsley, *Phys. Rev. B* **21**, 2717–33 (1980).
13. M. S. Whittingham, *Science* **192**, 1126–7 (1976).
14. E. A. Marseglia, *Int. Rev. Phys. Chem.* **3**, 177 (1983).
15. W. B. Davies, M. L. H. Green and A. J. Jacobsen, *J. Chem. Soc., Chem. Commun.* 781–2 (1976).
16. M. B. Dines, *Science* **1210** (1975).
17. R. P. Clement, W. B. Davies, K. A. Ford, M. L. H. Green and A. J. Jacobsen, *Inorg. Chem.* **17**, 2754 (1978).
18. S. Barlow, Part II thesis, Oxford (1992).
19. H. V. Wong and D. O'Hare, unpublished results (1992).
20. D. O'Hare, J. S. O. Evans, C. K. Prout and P. J. Wiseman, *Angew. Chem. Int. Ed. Engl.* **30**, 1156–1158 (1991).
21. L. Benes, J. Votinsky, P. Lostak, J. Kalousova and J. Klikorka, *Phys. Stat. Sol.* **89**, K1–K4 (1985).
22. H. Schäfer-Stahl and R. Abele, *Angew. Chem. Int. Ed. Engl.* **19**, 477–8 (1980).
23. T. R. Halbert and J. C. Scanlon, *Mat. Res. Bull.* **14**, 415–421 (1979).
24. W. Bunder and E. Weiss, *J. Organomet. Chem.* **92**, 65 (1975).
25. B. G. Silbernagel, M. B. Dines, F. R. Gamble, L. A. Gebhard and M. S. Whittingham, *J. Chem. Phys.* **65**, 1906–1913 (1976).
26. C. H. Holm and J. A. Ibers, *J. Phys. Chem.* **30**, 885 (1959).
27. S. J. Heyes, N. J. Clayden, C. M. Dobson, M. L. H. Green and P. J. Wiseman, *J. Chem. Soc., Chem. Commun.* 1560–62 (1987).
28. S. J. Heyes, D. Phil thesis, Oxford (1989).
29. S. J. Heyes, N. J. Clayden, M. L. H. Green, P. J. Wiseman and C. M. Dobson, manuscript in preparation.
30. S. J. Heyes, personal communication (1991).
31. C. A. Formstone, E. T. Fitzgerald, P. A. Cox and D. O'Hare, *Inorg. Chem.* **29**, 3860–3866 (1990).
32. C. A. Formstone, M. Kurmoo, E. T. Fitzgerald, P. A. Cox and D. O'Hare, *J. Mater. Chem.* **1**, 51 (1991).
33. C. P. Grey, J. S. O. Evans, D. O'Hare and S. J. Heyes, *J. Chem. Soc., Chem. Commun.* 1381 (1991).
34. B. G. Silbernagel, *Chem. Phys. Lett.* **34**, 298 (1975).
35. F. R. Gamble and A. H. Thompson, *Solid State Commun.* **27**, 379–82 (1978).
36. D. O'Hare, *Chem. Soc. Rev.* 121–126 (1992).
37. V. Ambegoaker, B. I. Halperin and J. S. Langer, *Phys. Rev. B* **4**, 2612 (1971).
38. H. Hahn and W. Klingen, *Naturwissenschaften* **52**, 494 (1965).
39. R. Clement, M. Doeuff and C. Gledel, *J. Chimie Phys.* **85**, 1053 (1988).
40. W. Klingen, R. Ott and H. Hahn, *Z. Anorg. Allg. Chem.* **396**, 271–8 (1973).

41. G. Ouvrard, R. Brec and J. Rouxel, *Mat. Res. Bull.* **20**, 1181–1189 (1985).
42. R. Brec, *Solid State Ionics* **22**, 3–30 (1986).
43. J. W. Johnson, in *Intercalation Chemistry*, eds. M. S. Whittingham and A. J. Jacobson (Academic Press, New York, 1982), pp. 267–283.
44. R. Clement, *J. Chem. Soc., Chem. Commun.* 647 (1980).
45. R. Clement and M. L. H. Green, *J. Chem. Soc. Dalton Trans.* 1566 (1979).
46. B. Bal, S. Ganguli and M. Bhattacharaya, *Physica B&C* **133**, 64–70 (1985).
47. J. P. Audiere, R. Clement, Y. Mathey and C. Mazieres, *Physica B* **99**, 133 (1980).
48. R. Clement, O. Garnier and Y. Mathey, *Nou. J. de Chimie* **6**, 13 (1982).
49. C. Sourisseau, J. P. Forgerit and Y. Mathey, *J. Phys. Chem. Solids* **44**, 119 (1983).
50. D. Glueck, *Inorg. Chem.*, in press.
51. R. Clement, O. Garnier and J. Jegoudez, *Inorg. Chem.* **125**, 1404–9 (1986).
52. M. Doeuff, C. Cartier and R. Clement, *J. Chem. Soc., Chem. Commun.* 629 (1988).
53. E. Prouzet, G. Ouvrard and R. Brec, *Mat. Res. Bull.* **21**, 195–200 (1986).
54. G. Ouvrard, R. Brec and J. Rouxel, *Comptes Rendus Acad. Sci. Paris* **294**, 971 (1982).
55. S. Soled and A. Wold, *Mat. Res. Bull.* **11**, 657 (1976).
56. Y. Mathey, A. Michalowicz, P. Taffoli and G. Vlaic, *Inorg. Chem.* **23**, 897–902 (1984).
57. K. Kurosawa, S. Saito and Y. Yamaguchi, *J. Phys. Soc. Japan* **11**, 3919–3926 (1983).
58. R. Clement, J. P. Audiere and J. P. Renard, *Rev. Chim. Miner.* **19**, 560 (1982).
59. A. Michalowicz and R. Clement, *J. Inclusion Phenomena* **4**, 256–71 (1986).
60. C. Berthier, Y. Chabre and M. Minier, *Solid State Commun.* **28**, 327–328 (1978).
61. R. Brec, D. M. Schleich, G. Ouvrard, A. Louisy and J. Rouxel, *Inorg. Chem.* **18**, 1814 (1979).
62. Y. Chabre, P. Segransan and C. Berthier, in *Fast Ion Transport in Solids*, eds. P. Vashishta, J. N. Mundy and G. K. Shenoy (North-Holland, Amsterdam, 1979), pp. 221–224.
63. R. Clement, H. Mercier and A. Michalowicz, *Rev. Chim. Miner.* **22**, 135 (1985).
64. Y. Mathey, R. Clement, C. Sourisseau and G. Lucazeau, *Inorg. Chem.* **19**, 2773–9 (1980).
65. C. Sourisseau, Y. Mathey and C. Poinsignon, *Chem. Phys.* **71**, 257–64 (1982).
66. D. A. Cleary and A. H. Francis, *J. Phys. Chem.* **89**, 97–100 (1985).
67. K. Kim, D. J. Little and D. A. Cleary, *J. Phys. Chem.* **94**, 3205–3210 (1990).
68. D. O'Hare, W. Jaegermann, D. L. Williamson, F. S. Ohuchi and B. A. Parkinson, *Inorg. Chem.* **27**, 1537–1542 (1988).
69. P. Hagenmuller, J. Rouxel and J. Partier, *Comptes Rendus Acad. Sci. Paris* **254**, 2000 (1962).
70. P. Hagenmuller, J. Portier, B. Barbe and P. Baudier, *Z. Anorg. Allg. Chemie* **355**, 209–217 (1967).
71. J. Rouxel and P. Palvadeau, *Rev. de Chimie Miner.* **19**, 317 (1982).
72. S. M. Kauzlarich and J. L. Stanton, Jr., *J. Am. Chem. Soc.* **108**, 7946–51 (1986).
73. S. M. Kauzlarich, B. K. Teo and B. A. Averill, *Inorg. Chem.* **25**, 1209–15 (1986).

74. J. F. Bringley and B. A. Averill, *J. Chem. Soc., Chem. Commun.* 399–400 (1987).
75. M. G. Kanatzidis, L. M. Tonge, T. J. Marks, H. O. Marcy and C. R. Kannewurf, *J. Am. Chem. Soc.* **109**, 3797 (1987).
76. M. G. Kanatzidis, M. Hubbard, L. M. Tonge, T. J. Marks, H. O. Marcy and C. R. Kannewurf, *Synth. Met.* **28**, C89 (1989).
77. M. G. Kanatzidis, H. O. Marcy, W. J. McCarthy, C. R. Kannewurf and T. J. Marks, *Solid State Ionics* **32/3**, 594–608 (1989).
78. H. Schäfer-Stahl, *Synth. Met.* **4**, 65 (1981).
79. H. Schäfer-Stahl, *Inorg. Nucl. Chem. Lett.* **16**, 271–6 (1980).
80. T. R. Halbert, D. C. Johnston, L. E. McCandlish, A. H. Thompson, J. C. Scanlon and J. A. Dumesic, *Physica B* **99**, 128 (1980).
81. G. Rousseau, *Comptes Rendus Acad. Sci. Paris* **110**, 1032 (1890).
82. M. S. Goldsztaub, *Comptes Rendus Acad. Sci. Paris* **198**, 667 (1934).
83. M. D. Lind, *Acta Cryst.* **B26**, 1058–62 (1970).
84. P. Palvadeau, J. P. Venien and G. Calvarin, *Comptes Rendus Acad. Sci. Paris* **292**, 1259 (1981).
85. H. Schäfer-Stahl and R. Abele, *Z. Anorg. Allg. Chem.* **465**, 147–52 (1980).
86. H. Schäfer-Stahl and R. Abele, *Mat. Res. Bull.* **15**, 1157–65 (1980).
87. P. Palvadeau, L. Coic and J. Rouxel, *Mater. Res. Bull.* **16**, 1055 (1981).
88. G. Villeneuve, P. Dordor, P. Palvadeau and J. P. Venien, *Mater. Res. Bull.* **17**, 1407 (1982).
89. P. Aldebert, N. Baffier, J.-J. Legendre and J. Livage, *Rev. Chim. Miner.* **19**, 485 (1982).
90. P. Turner and D. O'Hare, unpublished results (1992).
91. E. Rodriguez-Castellon, A. Jimenez-Lopez, M. Martinez-Lara and L. Moreno-Real, *J. Inclusion Phen.* **5**, 335 (1987).
92. G. E. Matsubayashi, S. Ohta and S. Okuno, *Inorg. Chimica. Acta* **184**, 47 (1991).
93. A. Davidson, G. Villeneuve, L. Fournes and H. Smith, *Mat. Res. Bull.* **27**, 357–65 (1992).
94. J. W. Johnson, *J. Chem. Soc., Chem. Commun.* 263–5 (1980).
95. K. Chatakondur, C. Formstone, M. L. H. Green, D. O'Hare, J. M. Twyman and P. Wiseman, *J. Mater. Chem.* **1**, 205–212 (1991).
96. A. M. Chippendale, P. G. Dickens and A. V. Powell, *Prog. Solid State Chem.* **21**, 133–198 (1991).
97. J. Legendre and J. Livage, *J. Colloid and Interface Sci.* **94**, 75–83 (1982).
98. J. Legendre, P. Aldebert, N. Baffier and J. Livage, *J. Colloid and Interface Sci.* **94**, 84–89 (1982).
99. P. Aldebert, H. Haesslin, N. Baffier and J. Livage, *J. Colloid and Interface Sci.* **98**, 478–483 (1984).
100. J. Livage, *Chem. Mater.* **3**, 578–593 (1991).
101. P. Aldebert and V. Paul-Boncour, *Mat. Res. Bull.* **18**, 1263 (1983).
102. B. Jordan and C. Calvo, *Can. J. Chem.* **51**, 2621–25 (1973).
103. J. W. Johnson, A. J. Jacobson, J. F. Brady and S. M. Rich, *Inorg. Chem.* **21**, 3820–25 (1982).
104. G. Matsubayashi and S. Ohta, *Chem. Lett.* 787 (1990).
105. H. Bräkken, *Z. Krist.* **78**, 484 (1931).
106. N. Wooster, *Z. Krist.* **80**, 504 (1931).
107. L. Kihlberg, *Arkiv. Kemi.* **21**, 357–64 (1963).
108. S. J. Mason, D. O'Hare, C. P. Grey, L. Bull and S. J. Heyes, *J. Mat. Chem.*, in press (1992).